Synergistic Catalytic Effect of Triple Dynamic Bonds for Fast-reprocessing and High-performance Cross-linked Polymers

Xiwei Xu,[a,c] Jiahui Wu,[d] Mingzhe Li,[d] Sheng Wang,[e] Hongzhi Feng,[a,c] Binbo Wang,[a,c] Kezhen Hu,[a,c] Chuanzhi Zhang,[a] Jin Zhu,[a] Songqi Ma[a,b]*

[a] Key laboratory of bio-based polymeric materials technology and application of Zhejiang province, Ningbo Institute of Materials Technology and Engineering, Chinese Academy of Sciences, Ningbo 315201, P. R. China

[b] School of Chemical and Material Engineering, Jiangnan University, Wuxi 214122, P. R. China

[c] University of Chinese Academy of Sciences, Beijing 100049, P. R. China

[d] Wanhua Chemical Group Co., Ltd., Yantai 264002, P. R. China

[e] Institute of Materials Research and Engineering, A*STAR (Agency for Science, Technology and Research), 2 Fusionopolis Way, Innovis, Singapore 138634, Singapore

*Corresponding authors: (Songqi Ma) E-mail songqi.ma@jiangnan.edu.cn

Contents

Experimental Section

Materials

All the raw materials, including *p*-aminophenyl disulfide (Aladdin, >98%), poly (propylene glycol) bis (2-aminopropyl ether) (D400, average $M_n \approx 400$, Aladdin), *p*-hydroxybenzaldehyde (Aladdin, 98%), aniline (Aladdin, >99.5%), *p*-toluidine (Aladdin, >99.7%), benzaldehyde (Aladdin, >99%), *p*-methyl benzaldehyde (Aladdin, >97%), hexyl isocyanate (Aladdin, >98%), phenyl disulfide (Aladdin, >99%), *p*-tolyl disulfide (Aladdin, >98%), hexamethylene diisocyanate trimer (Tri-HDI, Wanhua Chemical Group Co., Ltd., >99.0%), ethyl acetoacetate (EAA, Aladdin, >99%), guanidine carbonate (Aladdin, >99%), N,N'-carbonyldiimidazole (CDI, Aladdin, >97%), N, N'-dimethylformamide (DMF, Sinopharm, 99.5%), methanol (Sinopharm, 99.7%), ethanol (Sinopharm, 99.5%), acetone (Sinopharm, 99.5%) and dimethyl sulfoxide (DMSO, Sinopharm, 98%) were used without further purification.

Synthesis Protocols

Synthesis of diphenol monomer (DSOH)

DSOH was synthesized according to the literature.[1] In a 500-mL flask, 9.76 g (0.08 mol) of *p*-hydroxybenzaldehyde and 9.92 g (0.04 mol) of *p*-aminophenyl disulfide were dissolved in 200 mL of ethanol. The solution was stirred until it became transparent, and then the mixture was heated to 60 °C. After around 2 h of reaction at 60 °C, 12.65 g of light-yellow powder (DSOH, yield: 69.35%) was collected by suction filtration and drying in a vacuum oven at 80 °C for 4 h.
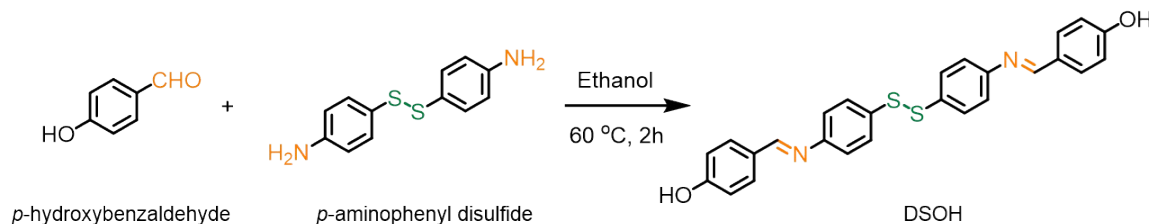
Scheme S1. Synthetic route of DSOH.

^{1}H NMR (600 MHz, DMSO-*d₆*, ppm, DSOH): δ = 10.17 (s, 1H), 8.47 (d, J = 12.0 Hz, 1H), 7.77 (t, J = 7.6 Hz, 2H), 7.52 (dd, J = 28.8, 8.4 Hz, 2H), 7.30-7.15 (m, 2H), 6.91 (dd, J = 30.9, 8.5 Hz, 2H).

^{13}C NMR (151 MHz, DMSO-*d₆*, ppm, DSOH): δ = δ 161.32 (s), 161.14 (s), 152.26 (s), 132.73 (s), 131.32 (s), 129.91 (s), 127.79 (s), 122.53 (s), 116.15 (s).

TOF-MS (ES⁺) m/z calculated for DSOH ($C_{26}H_{20}N_2O_2S_2$ (M⁺ H⁺)): 457.

Synthesis of diamine monomer ((UPy-NH₂)-x)

(UPy-NH₂)-x was synthesized referring to the literature.[2, 3] In a 500-mL flask, the suspensions of 6.51 g (0.05 mol) EAA and 6.66 g (0.055 mol) guanidine carbonate were refluxed overnight in 300 mL of dry ethanol. The reaction liquid was then cooled, and the precipitate was filtered and washed with ethanol, water, and acetone to get white powder (MIC,

5.21 g, yield: 83.36%). In a 1000-mL flask, 8.00 g (0.064 mol) of MIC and 14.58 g (0.090 mol) of CDI were suspended in 400 mL DMSO, following stirred at 80 °C for approximately 15 min, the solution turned transparent. Then, after reaction at 80 °C for approximately 2 h, a substantial quantity of white powder was produced. The precipitate was filtered, washed with ethanol, and dried at 80 °C for 4 h to get 9.31 g of white powder (MIC-CDI, yield: 53.14%). In addition, 2.00 g (0.0091 mol) of MIC-CDI and 10.92 g (0.0273 mol) of D400 were combined in a 100-mL flask and stirred at 40 °C. After about 1 hour of reaction, the mixture became clear, and after 12 h of reaction at 40 °C, a viscous, translucent liquid termed (UPy-NH$_2$)-20% was obtained. (UPy-NH$_2$)-10% and (UPy-NH$_2$)-30% were produced in the same manner as (UPy-NH$_2$)-20%.
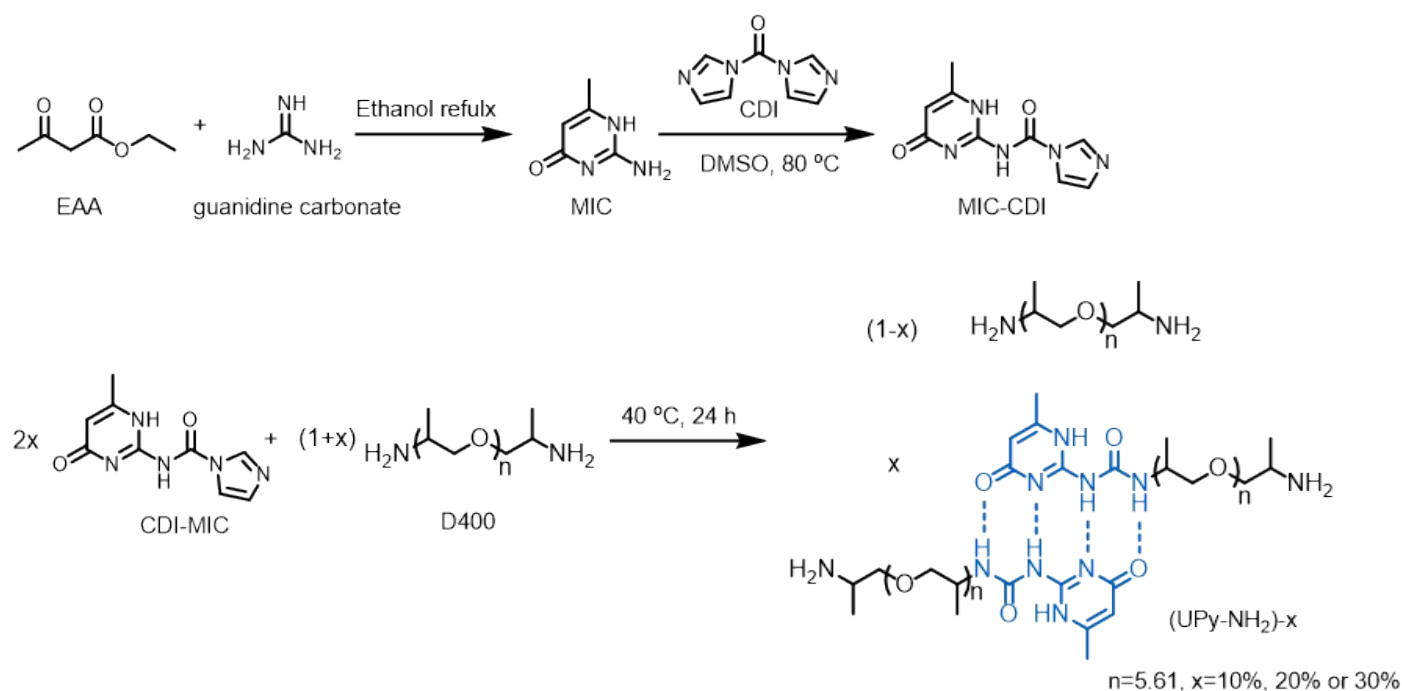
Scheme S2. Synthetic route of (UPy-NH$_2$)-x.

^{1}H NMR (600 MHz, DMSO-d_6, ppm, MIC): δ = 10.78 (s, 1H), 6.55 (s, 2H), 5.39 (s, 1H), 1.99 (s, 3H).

^{13}C NMR (151 MHz, DMSO-d_6, ppm, MIC): δ = 166.70 (s), 163.32 (s), 155.89 (s), 100.59 (s), 24.10 (s).

TOF-MS (ES$^+$) m/z calculated for MIC (C$_5$H$_7$N$_3$O (M$^+$ H$^+$)): 126.

Synthesis of CO. 1 and CO. 2

CO. 1 and CO. 2 were prepared by the dehydration condensation reaction of amino groups and aldehyde groups. Take the preparation of CO. 1 as an example, in a 250-mL flask, 5.31 g (0.05 mol) of benzaldehyde and 4.65 g (0.05 mol) of aniline were dissolved in around 100 mL ethanol. After heating at 60 °C for 2 h and rotary evaporation to remove part of the solvent (ethanol), a substantial quantity of light-yellow powder was produced. The precipitate was filtered, washed with ethanol and dried in a vacuum oven at 80 °C for 4 h to get a light-yellow powder (CO. 1, 6.39 g, yield: 70.61%). CO. 2 was synthesized by the similar method using *p*-toluidine and *p*-methyl benzaldehyde as the raw materials.
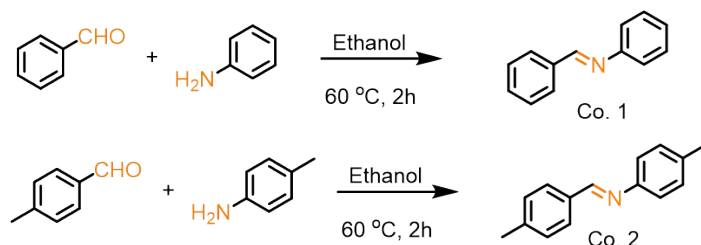
Scheme S3. Synthetic routes of CO. 1 and CO. 2.

^{1}H NMR (600 MHz, DMSO-d_6, ppm, CO. 1): δ = 8.62 (s, 1H), 7.95 (dd, J = 7.3 Hz, 2H), 7.60-7.48 (m, 3H), 7.48-7.34 (m, 2H), 7.26 (t, J = 7.9 Hz, 3H).

^{13}C NMR (151 MHz, DMSO-d_6, ppm, CO. 1): δ = 161.17 (s), 151.95 (s), 136.50 (s), 131.95 (s), 129.65 (d, J = 6.7 Hz), 129.31 (d, J = 6.3 Hz), 129.15 (s), 126.44 (s), 121.44 (s).

TOF-MS (ES$^+$) m/z calculated for CO. 1 (C$_{13}$H$_{11}$N (M$^+$ H$^+$)): 182.

^{1}H NMR (600 MHz, DMSO-d_6, ppm, CO. 2): δ = 8.57 (s, 1H), 7.82 (d, J = 8.0 Hz, 2H), 7.32 (d, J = 7.9 Hz, 2H), 7.19 (q, J = 8.3 Hz, 4H), 2.38 (s, 3H), 2.32 (s, 3H).

^{13}C NMR (151 MHz, DMSO-d_6, ppm, CO. 2): δ = 159.93 (s), 149.41 (s), 141.74 (s), 135.61 (s), 134.11 (s), 130.14 (s), 129.86 (s), 129.03 (s), 121.37 (s), 21.62 (s), 21.04 (s).

TOF-MS (ES$^+$) m/z calculated for CO. 2 (C$_{15}$H$_{15}$N (M$^+$ H$^+$)): 210.

Synthesis of HPU

HPU was synthesized by an addition reaction between amino group and isocyanate. In a 250-mL flask, 9.31 g (0.10 mol) of aniline and 12.71g (0.10 mol) of hexyl isocyanate were dissolved in around 150 mL chloroform. After reacting at 60° C for 4 h, the reacted solution was cooled to 0 °C, where snowflake-like crystals formed as a result. A bright-yellow solid was formed by filtering the precipitate, dissolving it in chloroform again, and then adding the solution dropwise to petroleum ether. Light-yellow crystals (HPU, 0.91 g, yield: 41.36%) were obtained by drying the precipitate at 80 °C for 4 h.
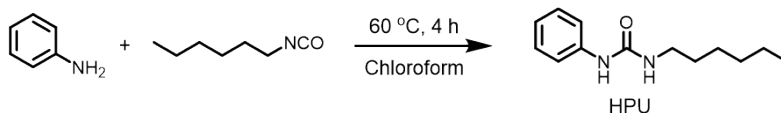
Scheme S4. Synthetic route of HPU.

^{1}H NMR (600 MHz, DMSO-d_6, ppm, HPU): δ = 8.55-8.20 (m, 1H), 7.52-7.29 (m, 2H), 7.20 (t, J = 7.9 Hz, 2H), 6.96-6.73 (m, 1H), 6.09 (d, J = 4.9 Hz, 1H), 3.17-2.91 (m, 2H), 1.57-1.34 (m, 2H), 1.34-1.10 (m, 6H), 1.00-0.70 (m, 3H).

^{13}C NMR (151 MHz, DMSO-d_6, ppm, HPU): δ = 155.65 (s), 141.09 (s), 129.07 (s), 121.32 (s), 118.00 (s), 39.48 (s), 31.50 (s), 30.19 (s), 26.52 (s), 22.56 (s), 14.39 (s).

Preparation of dynamic cross-linked polymers (DCPs: 0%UPy, 10%UPy, 20%UPy and 30%UPy)

The dynamic cross-linked polymers were prepared through a one-pot, one-step process involving reactions of hydroxyl groups and amino groups with isocyanates. Here, the preparation process of 20%UPy was taken as an example. 3.36 g (0.0067 mol, 0.02 mol -NCO) of hexamethylene diisocyanate trimer (Tri- HDI), 2.28 g (0.005 mol, 0.01 mol -OH) of DSOH and 2.70 g (0.005 mol, 0.01 mol -NH$_2$) of (UPy-NH$_2$)-20% were dissolved in around 20 mL N, N'-dimethylformamide and stirred quickly. Then the solution was placed in a vacuum oven, and the solvent was evaporated at 100 °C, 50 KPa for 15 min. Heated until the solvent was almost completely volatilized to get the pre-cured films, and then the pre-cured film was post-cured at 100 °C, 120 °C and 150 °C, <1 KPa for 1 hour to prepare dynamic cross-linked polymer. Through the above method, 0%UPy, 10%UPy and 30%UPy can be prepared by using D400, (UPy-NH$_2$)-10% and (UPy-NH$_2$)-30% instead of (UPy-NH$_2$)-20%.

Characterization Techniques

Gel contents

The cured samples (0.08-0.1 g) were weighed after drying at 80 °C in vacuum oven for 12 h, and recorded the initial weight as W_1. A Soxhlet extractor was used to extract the cured samples by acetone for 48 h, then they were vacuum dried for 12 h at 80 °C and weighed again (W_2). Gel contents were determined as equation S1:

$$100\% \times W_2/W_1 \tag{S1}$$

Swelling test

Approximately 50 mg of the cured samples were weighed and recorded as W_i before being soaked in various organic solvents (methane, ethane, acetone, THF, chloroform and DMF, approximately 20 mL) at room temperature for 48 h. The solvent on the surface of the samples was fully wiped away using absorbent cotton, and then the samples were weighed and recorded as W_f. The swelling ratios were determined as equation S2:

$$100\% \times (W_f - W_i) / W_i \tag{S2}$$

Dynamic mechanical analysis

a. Dynamic mechanical properties

   Dynamic mechanical properties were performed on a Q800 DMA (TA instruments, America) using a multi-frequency strain mode to get the storage modulus, loss modulus, and tan delta. The temperature was ramped from -10 °C to 200 °C with a constant ramp rate of 3 °C min^{-1} at a set frequency of 1 Hz, and the cross-link density (v_e) of the cured samples was calculated using equation S3:

$$E'=3v_eRT \tag{S3}$$

b. Stress relaxation

Stress relaxation test was conducted *via* a Q800 DMA (TA instruments, America) using a stress relaxation mode. The samples were examined between 150 °C and 180 °C by applying a constant strain of 2%. Before the tests, all the samples were held at the test temperatures (150 °C, 160 °C, 170 °C, and 180 °C) for 5 min to achieve thermal equilibrium and preloaded a 1×10^{-3} N force to prevent the samples from bending.

c. Calculation of activation energies (E_as)

The method described in the literature was used to calculate activation energies (E_as) [4, 5]. The typical stress relaxation time (τ^*) was obtained, at the time when the stress relaxation modulus dropped to 1/e of the original modulus. The stress relaxation activation energies (E_as) were determined by applying the Arrhenius law to the observed stress relaxation time and the matching temperature as follow:

$$\tau^*(T) = \tau^*_0 e^{E_a/RT} \quad (R = 8.314 \text{ J K}^{-1} \text{ mol}^{-1}) \qquad \text{(S4)}$$

d. Creep resistance

Creep resistance were performed on a Q800 DMA (TA instruments, America). The samples were exposed to a constant stress of 1 MPa for 10 min at the test temperature (30 °C, 80 °C, 100 °C, and 120 °C), after which the tension was removed and a 30-minute recovery period was conducted. The strain of the sample was recorded throughout this process. Besides, tensile creep time-temperature superposition (TTS) tests were carried out at temperatures ranging from 20 °C to 120 °C in 10 °C increments. During the process of measuring each isotherm, a steady stress of 2 MPa was applied for 10 min, and then there was a 10-minute recovery period after that.

Rheology studies

Rheology tests were performed on a HR-3 rotating rheometer (TA instruments, America) fitted with parallel plate geometry (25 mm in diameter) using a frequency sweeps mode under N_2 environment. The axial force was maintained at roughly 5 N throughout the experiment by using the axial force controller. Frequency sweeps were performed from 0.01 to 500 rad s^{-1} at 180 °C with a constant strain amplitude of 2%.

Exchange experiments of model compounds

Exchange experiments were carried out through the interaction and synergistic catalytic effect of the monomers containing imine bonds (CO. 1 and CO. 2), disulfide bonds (phenyl disulfide and *p*-tolyl disulfide), and urea groups (HPU). 0.091 g (5×10^{-4} mol) of CO. 1 and 0.105 g (5×10^{-4} mol) of CO. 2 were dissolved into 50 mL DMSO, and reacted at 50 °C for 10, 20, 30 or 100 min. 0.5 mL of the reaction solution was added to 1 mL of chloroform and mixed well, and the ratio of each component was detected by GC-MS. By dissolving 0.109 g (5×10^{-4} mol) of phenyl disulfide and 0.123 g (5×10^{-4} mol) of p-tolyl disulfide or 0.011 g (5×10^{-5} mol) of HPU or 0.109 g (5×10^{-4} mol) of phenyl disulfide, 0.123 g (5×10^{-4} mol) of p-tolyl disulfide and 0.011 g (5×10^{-5} mol) of HPU in DMSO, following the same method above,

the efficiency of imine exchange with the addition of the catalytic system can be obtained.
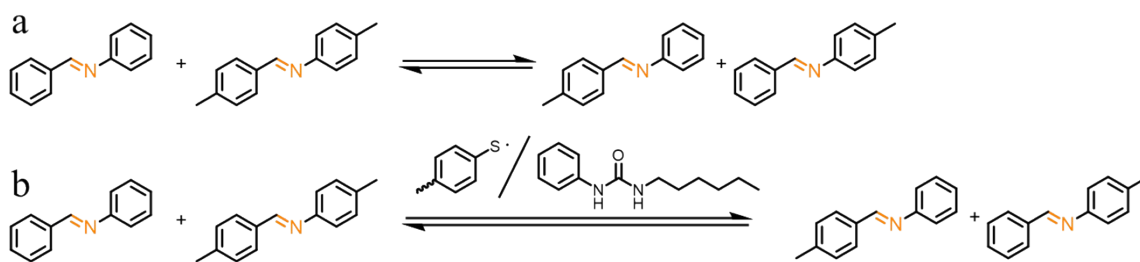
Scheme S5. Imine exchange (a) without and (b) with catalyst.

Reprocessing experiments

A flat vulcanizer was used to conduct the reprocessing experiments. Between two flat steel sheets covered with polyimide films, around 5 g of broken or used samples (containing 0% UPy, 10% UPy, 20% UPy, and 30% UPy) were inserted. Then it was pressed for 10 min at 160 °C, 10 MPa. For additional test, the reprocessed samples were sliced into rectangular shape.

Preparation of CF/DCP composites.

A flat vulcanizer was used for the preparation of CF/DCP composites. Three pieces of carbon fiber sheets weighting 5 g totally were stacked and covered by two DCP (20% UPy) films weighting 15 g totally. The above samples were placed between two steel plates covered with polyimide films and preheated at 160 °C for around 10 min, and gradually pressurized and degassed for 1 min and pressed at 160 °C and 2 MPa for 10 min, then hot pressed at 160 °C and 10 MPa for 30 min. The prepared samples were cold-pressed at 10 MPa for another 10 min to obtain CF/DCP composites.

Characterization

DMSO-d_6 was used as the solvent for ^{1}H NMR (600 MHz) and ^{13}C NMR (150 MHz) experiments on an AVANCE NEO Bruker NMR spectrometer (Bruker, Switzerland). Time-of-flight mass spectrometry was done in positive ion mode on an AB Sciex Triple TOF 4600 time-of-flight mass spectrometer (AB Sciex, America), DSOH and MIC were dissolved in dichloromethane; CO. 1 and CO. 2 were dissolved in methane. For the sake of examining the glass transition temperatures (T_gs) of the DCPs, differential scanning calorimetry (DSC) were used on a Mettler-Toledo Star 1 apparatus. The DCPs (approximately 5 mg) were heated at a rate of 20 °C min^{-1} from 25 °C to 180 °C, kept at 180 °C for 3 min to erase thermal history, then cooled to 0 °C at a rate of 20 °C min^{-1} from 180 °C, and the T_gs of the DCPs were calculated using the second heating curves. On a 7890B-5977A Gas Chromatography-mass Spectrometer (Agilent, America), GC-MS spectra were obtained. On a Mettler-Toledo TGA/DSC1 thermogravimetric analyzer (Mettler Toledo, Switzerland), thermogravimetric analysis (TGA) of the DCPs (about 5 mg) was carried out from 50 to 800 °C at a rate of 10 °C min^{-1} in a N$_2$/air atmosphere. On a Micro-FT IR Cary660 (Agilent, America), the FT-IR spectra were obtained in absorbance

mode. An Instron 5567 Electric Universal Testing Machine (Instron, America) was used to perform the tensile tests. The samples were measured with a gauge length of 15 mm and a cross-head speed of 2 mm min^{-1}, with results averaged from at least 5 specimens for accuracy.

Theoretical Calculations

a. *"DFT"* analysis

All calculations were carried out with the Gaussian 16 program. The initial model of the reactants, intermediates, and final products involved in the initial reaction was structurally optimized with the B3LYP-D3 functional[6-8], and the 6-311G+(2d,2p) basis set[9] were used to find the most stable geometry and then search for related reactants in the transition state. For the corresponding product, the transition state has only an imaginary frequency, and the reactants, intermediates, and products have no imaginary frequency. The transition state is followed by the TS method in two directions following the intrinsic reaction coordinate (IRC) analysis to ensure that the transition state is related to the correct reactants and products. Frequency analysis and IRC analysis were performed using the same basis set as the optimization.

b. Moldex 3D

The filling and infiltration process of preparation of CF/DCP composites was simulated by Moldex 3D software. Firstly, the model with fiber sheet and boundary condition (10 cm × 10 cm × 3 mm) were prepared in Moldex3D Mesh. The upper and surrounding surface of model was set as inlet and vent separately, and the material for melt and ply was selected in material wizard. The filling process was controlled by pressure and the maximum inlet pressure was set as 10 MPa. According to the viscosity performance, the resin and mold temperature was controlled at 160 °C. After setting, the simulation can be submitting to calculate and confirming whether or when the cavity can be completely filled. After finishing analysis, the filling time was extracted to perform the filling status.

Characterization of small model compounds
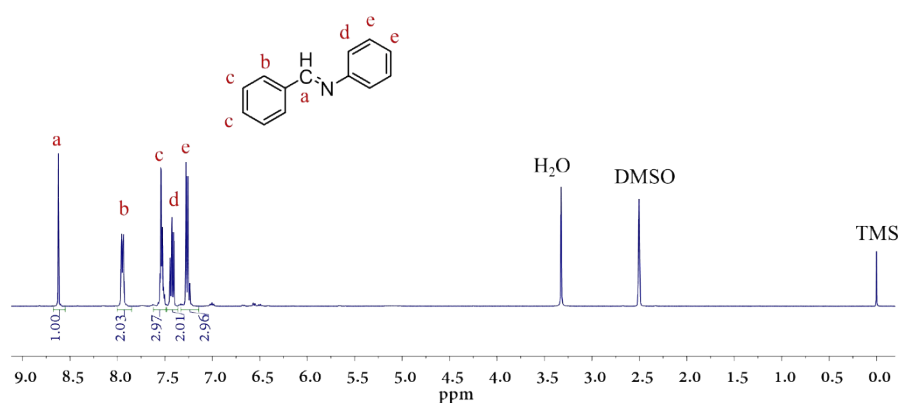
Figure S1. ^{1}H NMR spectrum of DMI.
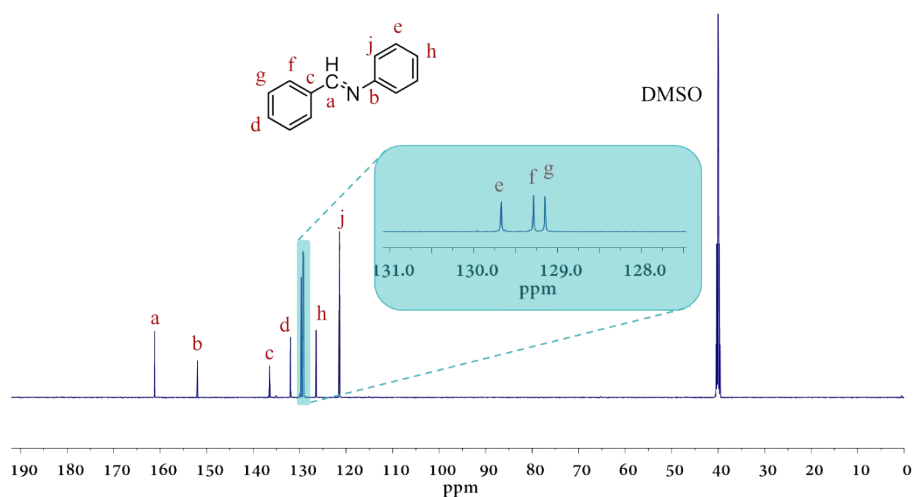
Figure S2. ^{13}C NMR spectrum of DMI.
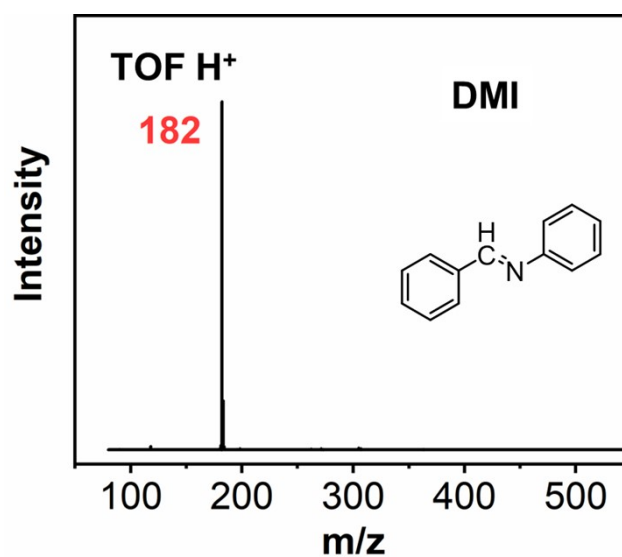
Figure S3. TOF-MS spectrum of DMI.
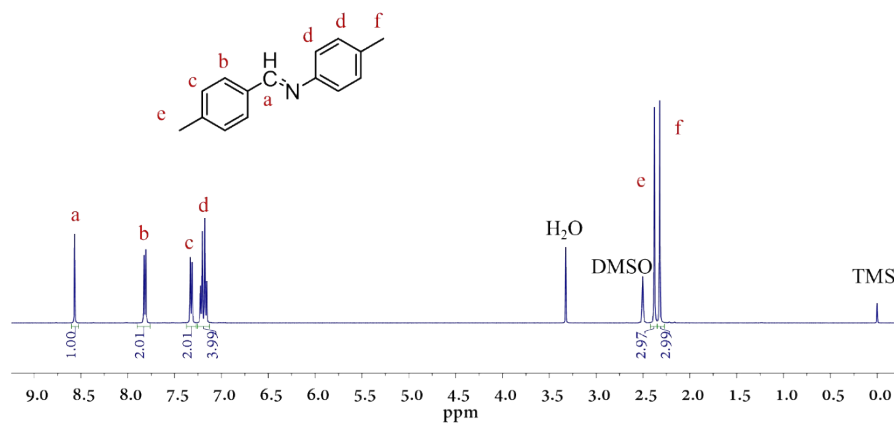
Figure S4. ^{1}H NMR spectrum of DTMI.
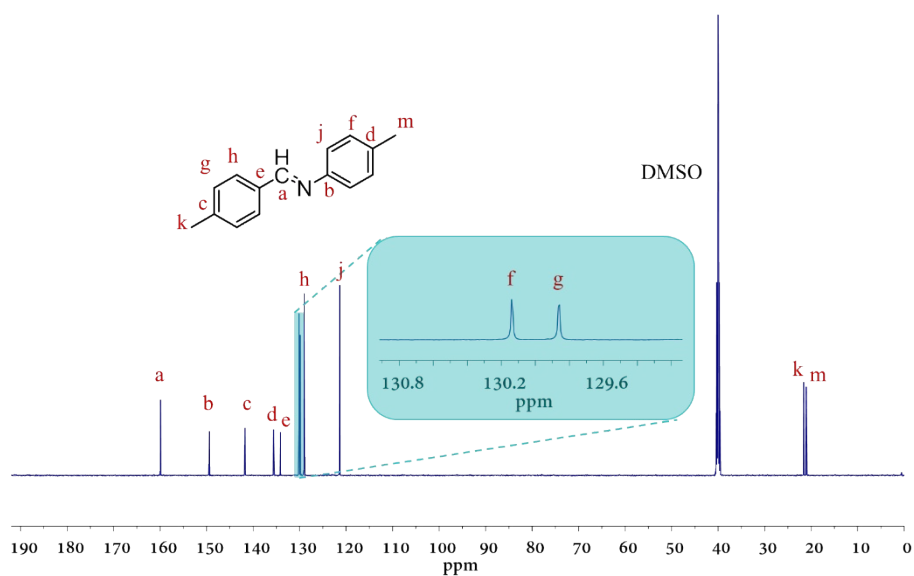
Figure S5. ^{13}C NMR spectrum of DTMI.
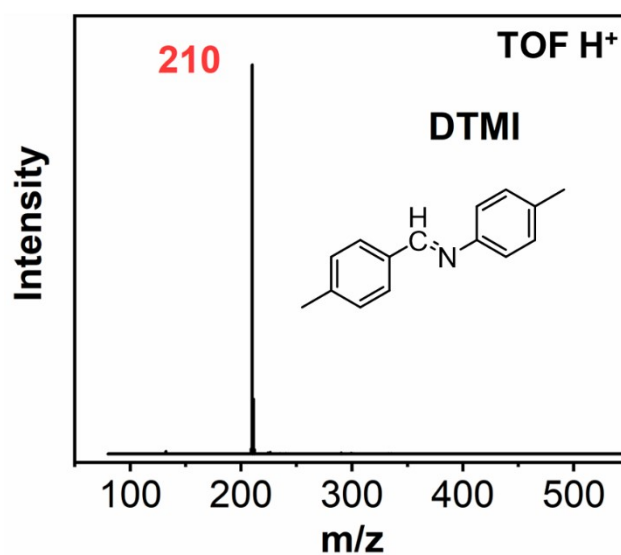
Figure S6. TOF-MS spectrum of DTMI.
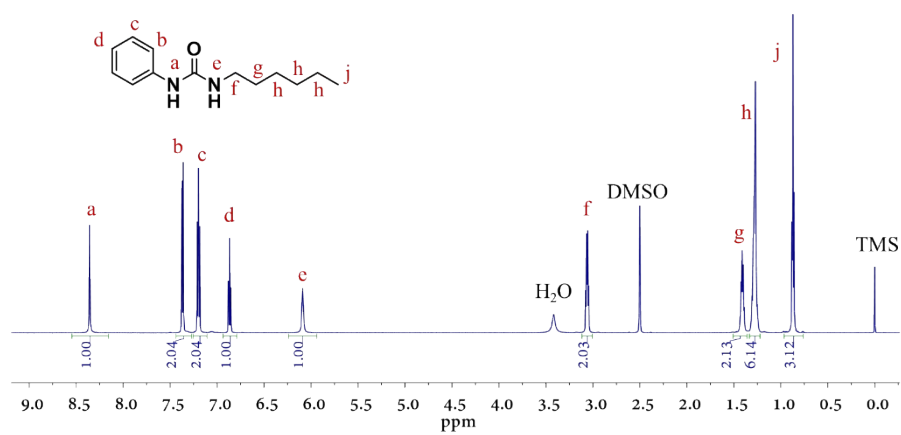
Figure S7. ^{1}H NMR spectrum of HPU.

10
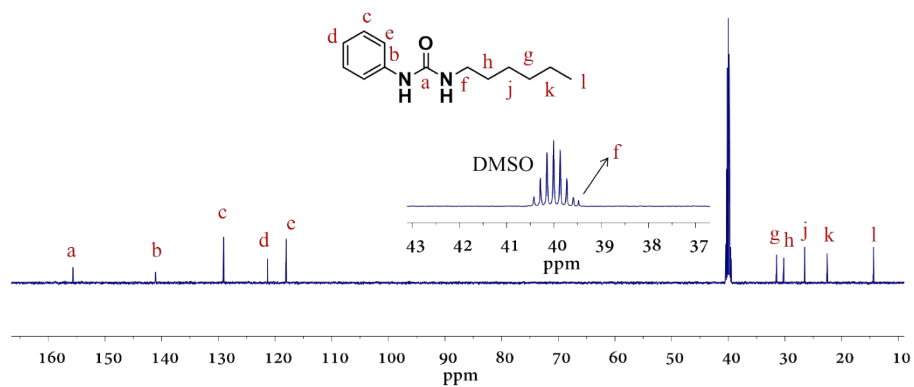
Figure S8. ^{13}C NMR spectrum of HPU.
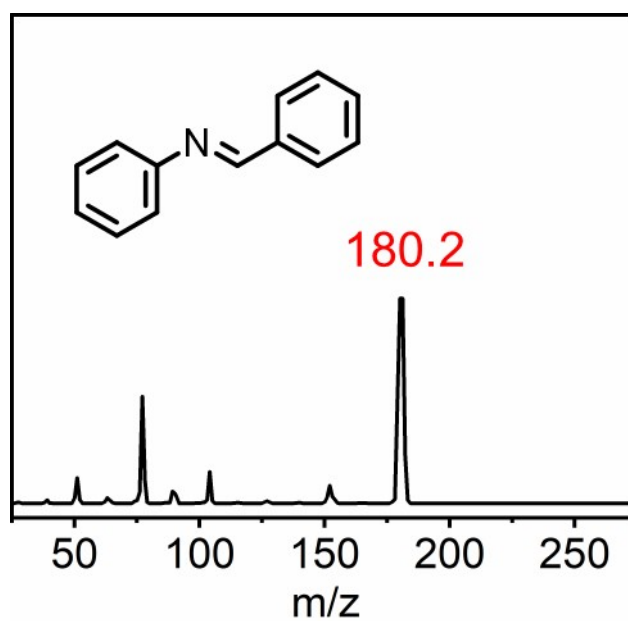
Figure S9. MS spectrum of DMI at the retention time of around 15.4 min.
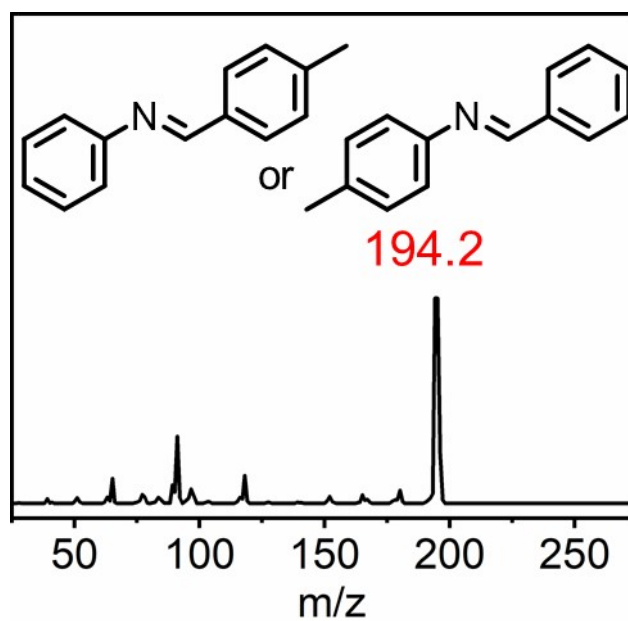
Figure S10. MS spectrum of Co.2 or Co.3 at the retention time of around 16.3 min.
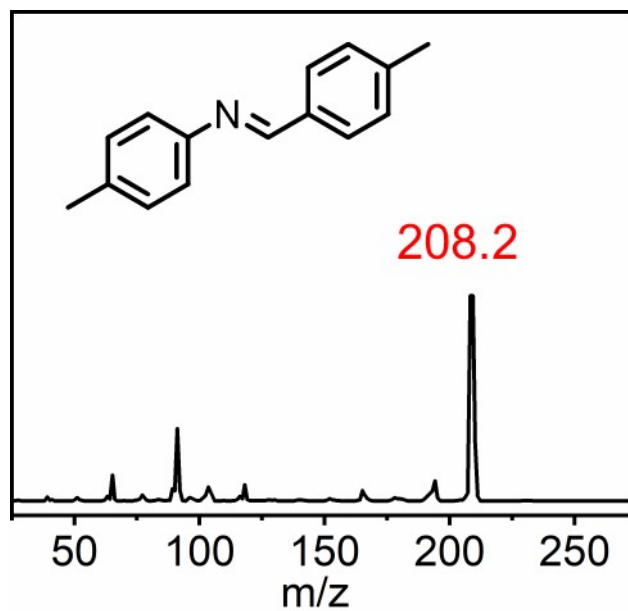
Figure S11. MS spectrum of DTMI at the retention time of around 17.1 min.
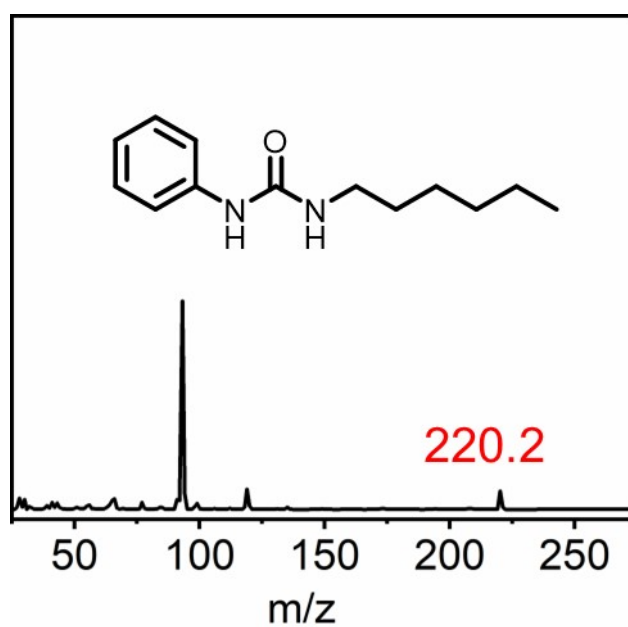
Figure S12. MS spectrum of HPU at the retention time of around 18.1 min.
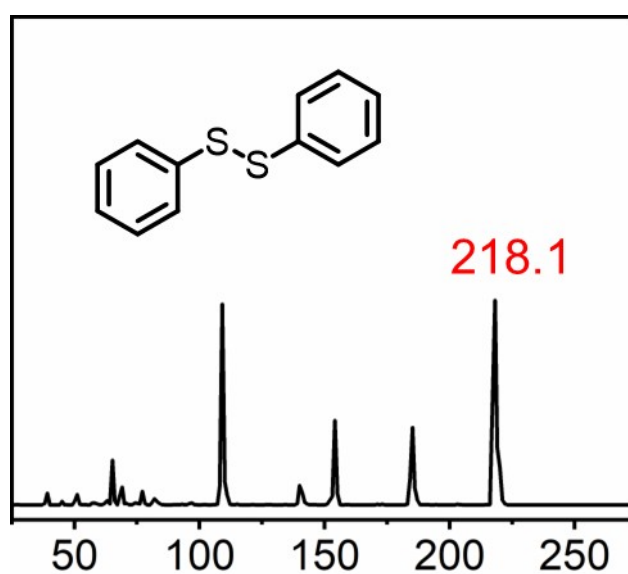
Figure S13. MS spectrum of phenyl disulfide at the retention time of around 16.6 min.
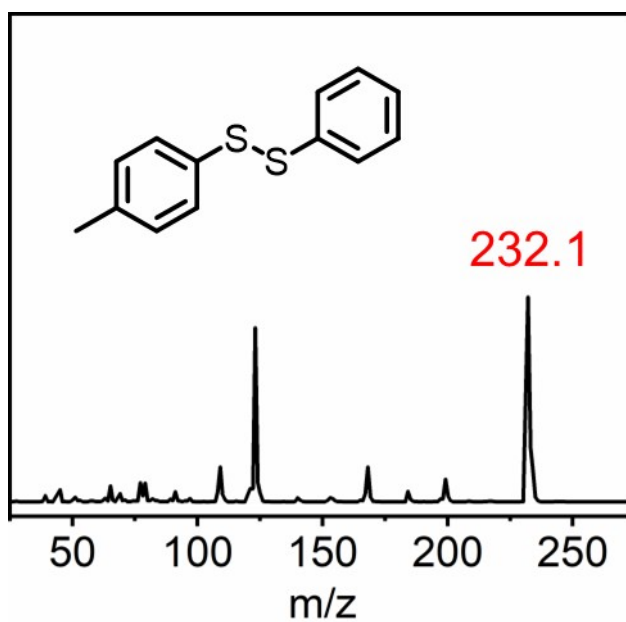
Figure S14. MS spectrum of phenyl-*p*-tolyl disulfide at the retention time of around 17.3 min.
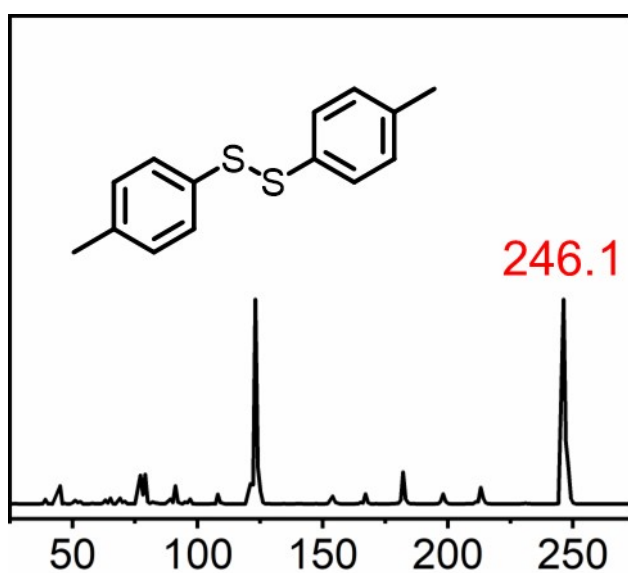
Figure S15. MS spectrum of phenyl disulfide at the retention time of around 18.0 min.

Supplementary Characterization Data for DCPs
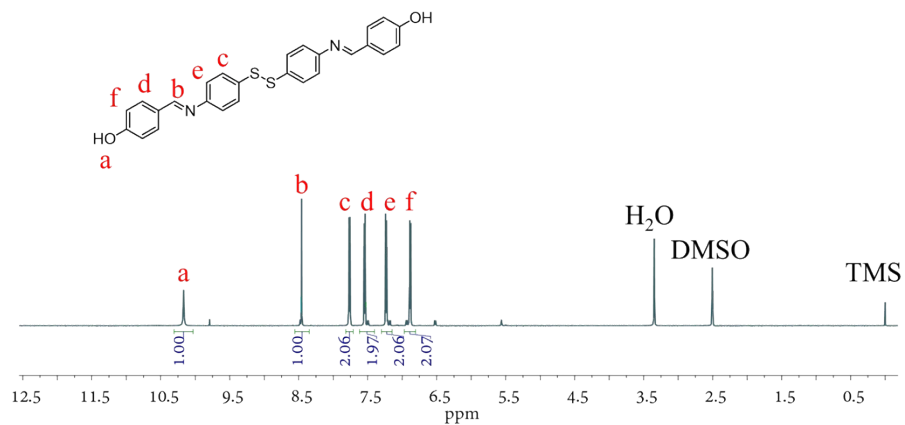
Figure S16. ^{1}H NMR spectrum of DSOH.
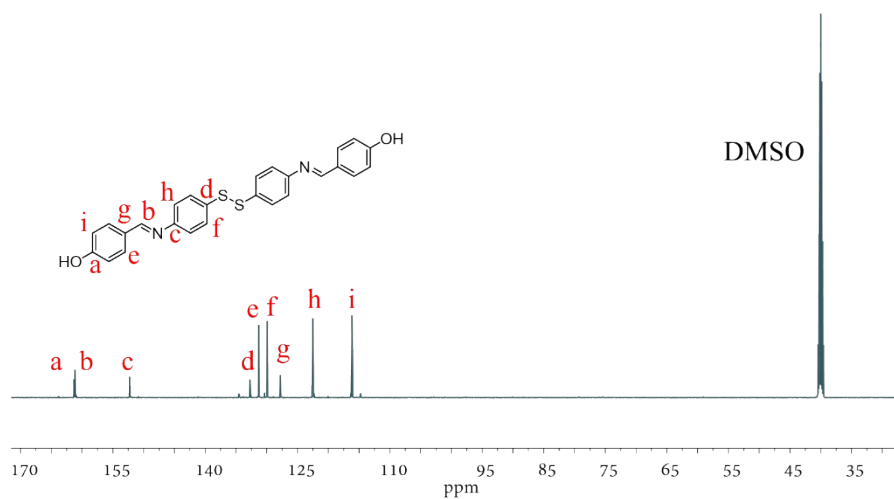
Figure S17. ^{13}C NMR spectrum of DSOH.
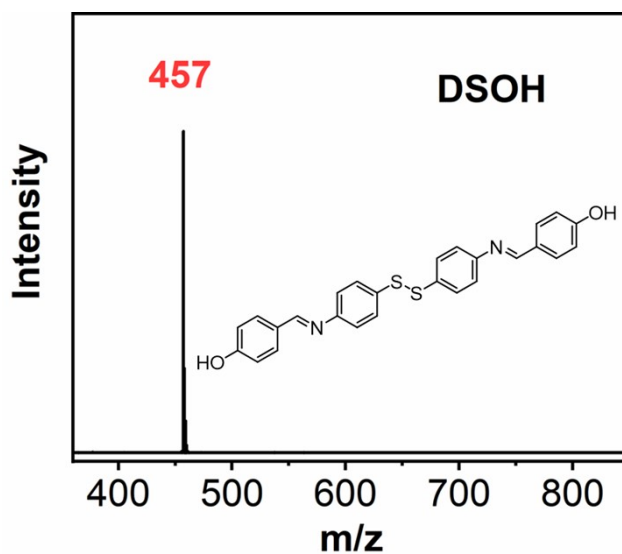
Figure S18. TOF-MS spectrum of DSOH.
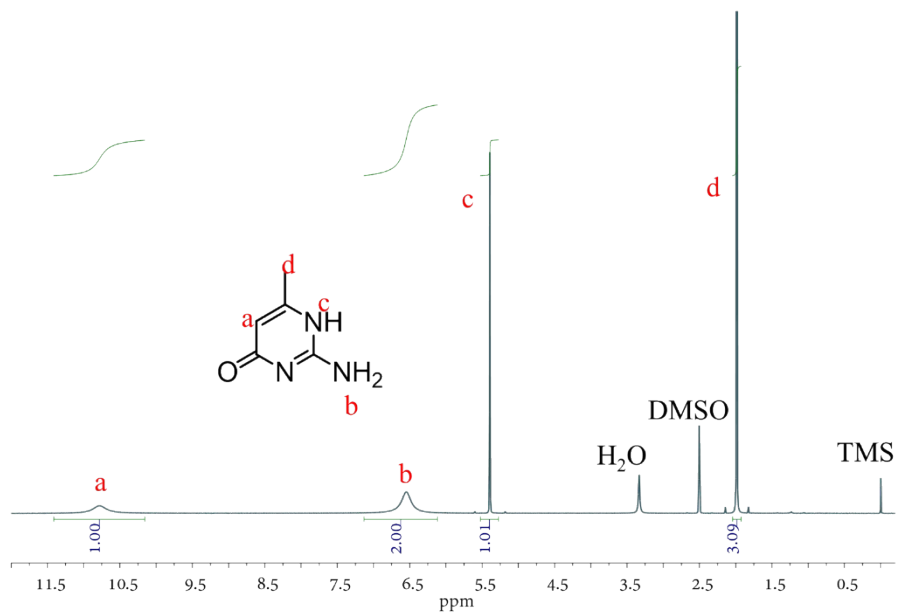
Figure S19. ^{1}H NMR spectrum of MIC.
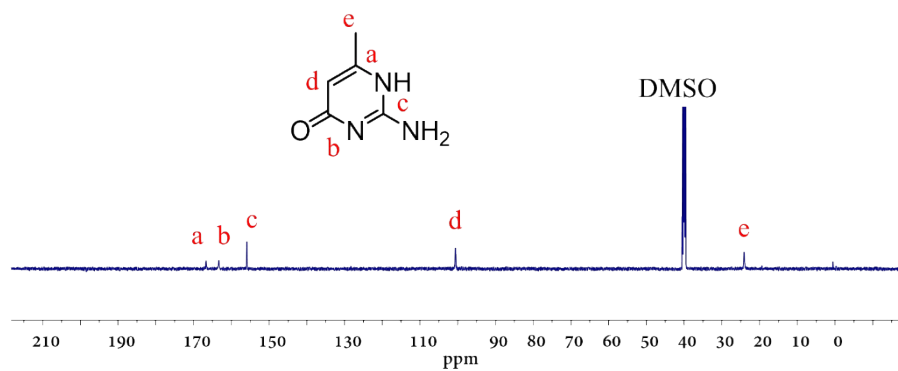
Figure S20. ^{13}C NMR spectrum of MIC.
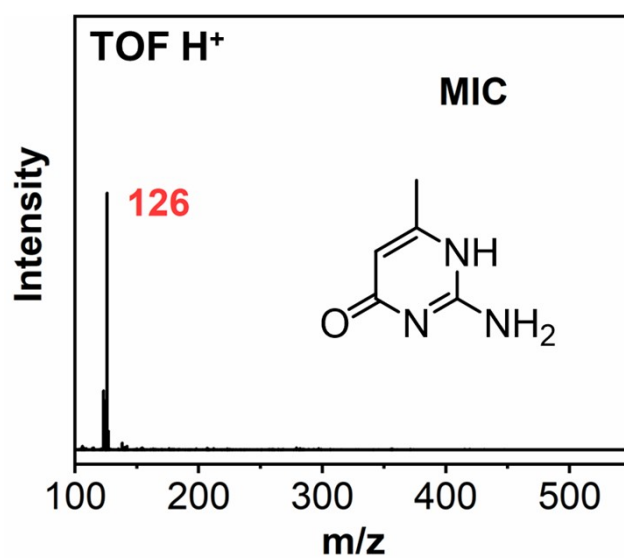
Figure S21. TOF-MS spectrum of MIC.

15
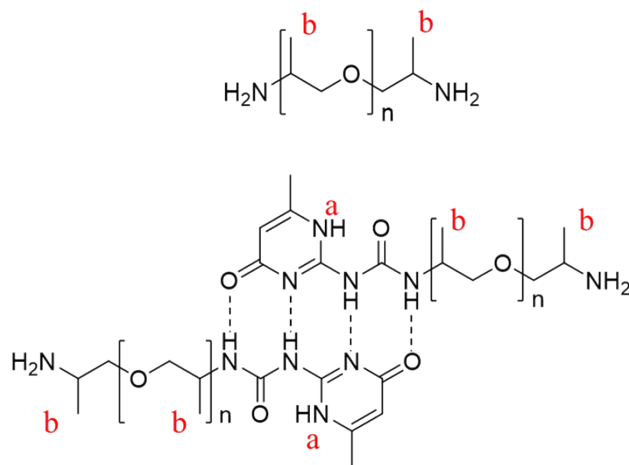
Figure S22. Chemical structure of UPy-x
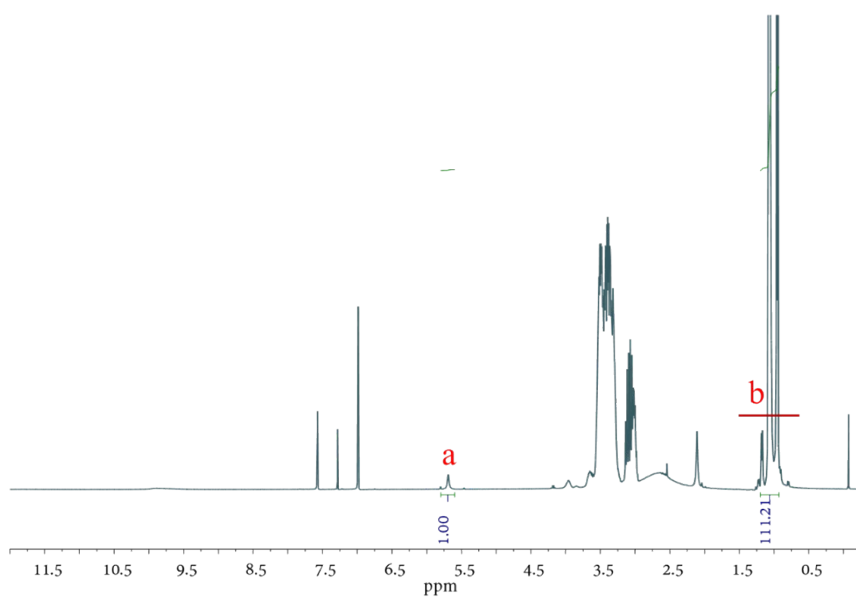
Figure S23. ^{1}H NMR spectrum of UPy-10%.
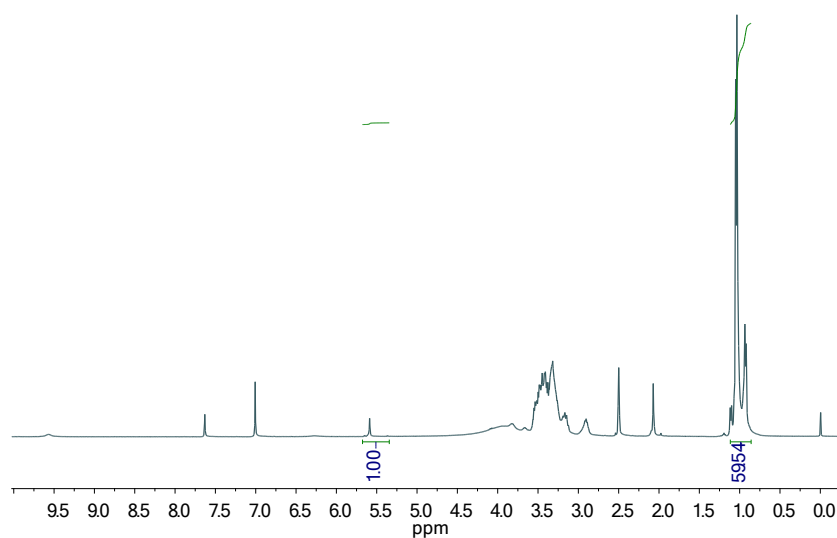
Figure S24. ^{1}H NMR spectrum of UPy-20%.
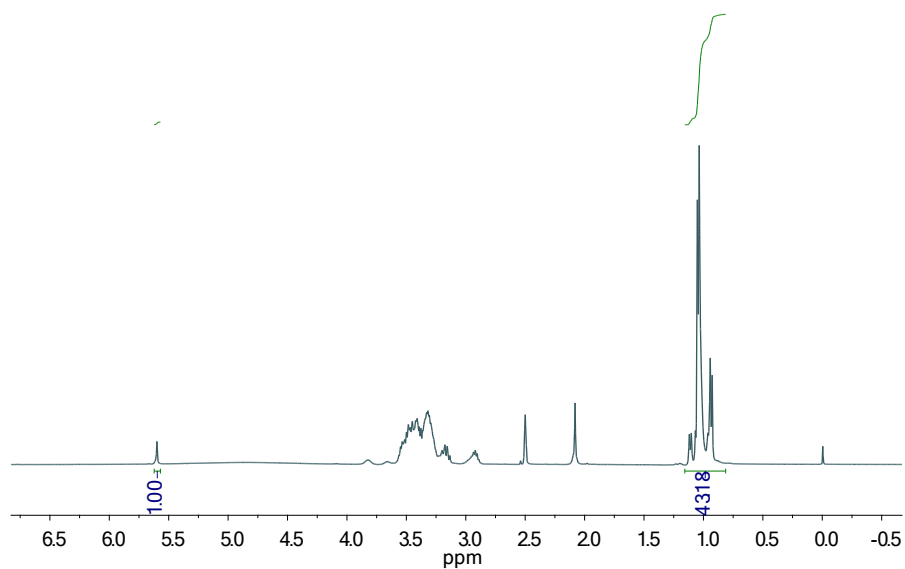
Figure S25. ^{1}H NMR spectrum of UPy-30%.
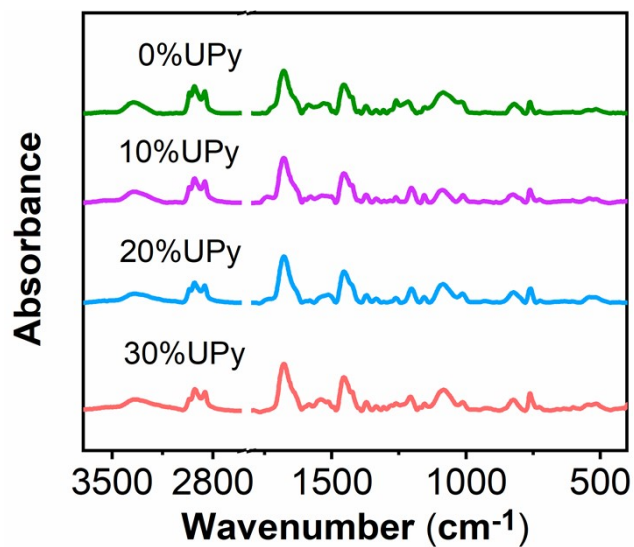
Figure S26. FT-IR spectrum of DCPs.
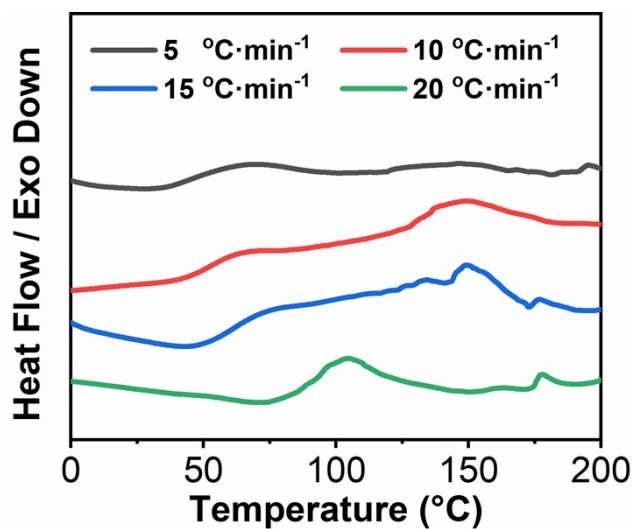
Figure S27. DSC curves of non-isothermal curing for 0%UPy system at different heating rates.
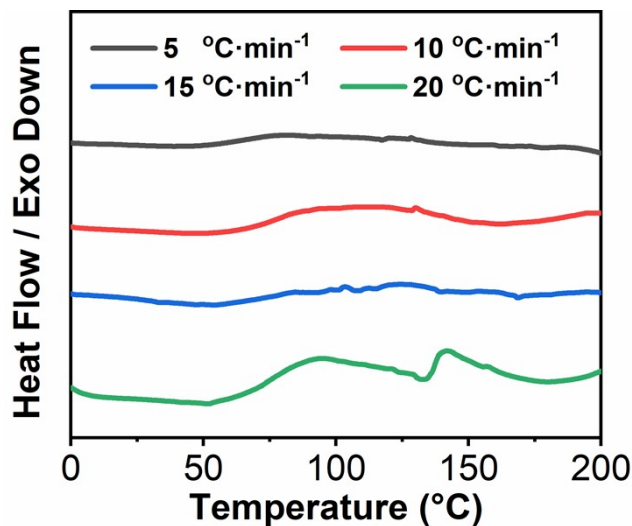
Figure S28. DSC curves of non-isothermal curing for 10%UPy system at different heating rates.
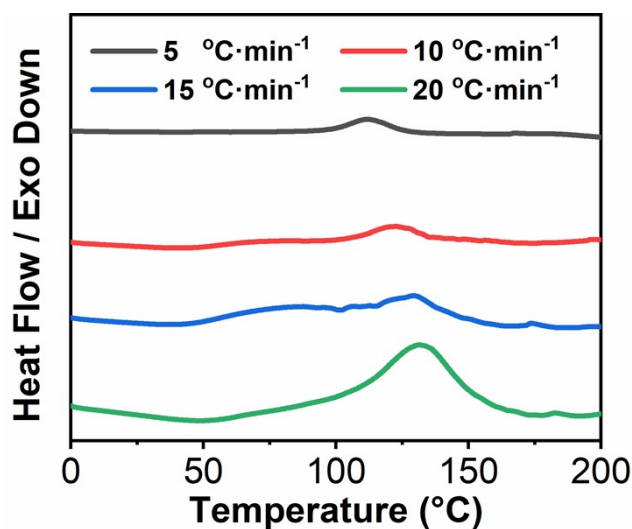
Figure S29. DSC curves of non-isothermal curing for 20%UPy system at different heating rates.
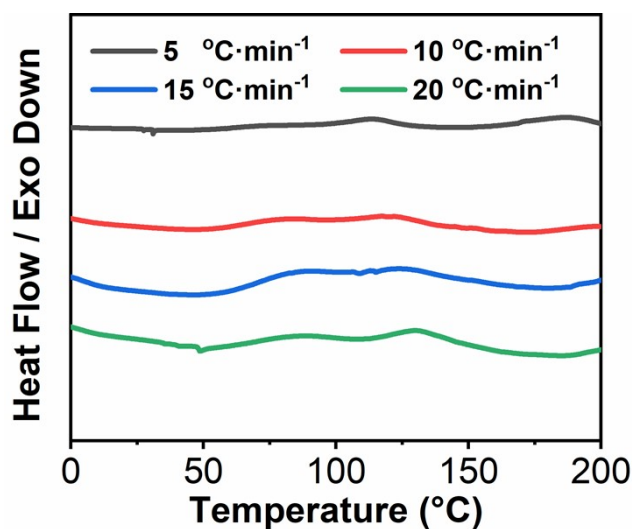
Figure S30. DSC curves of non-isothermal curing for 30%UPy system at different heating rates.
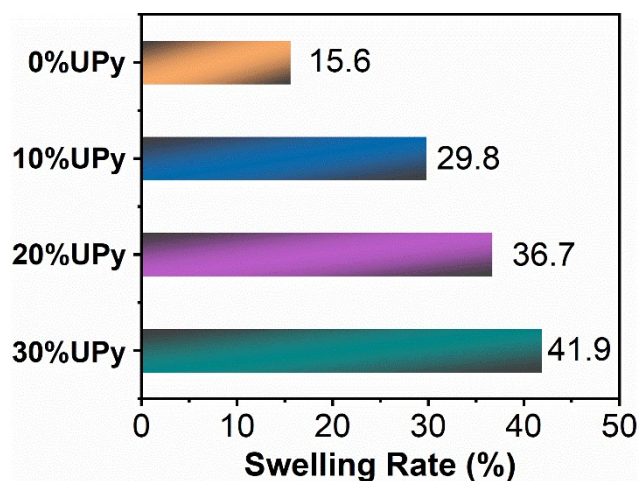
Figure S31. Swelling ratios of the DCPs in THF.
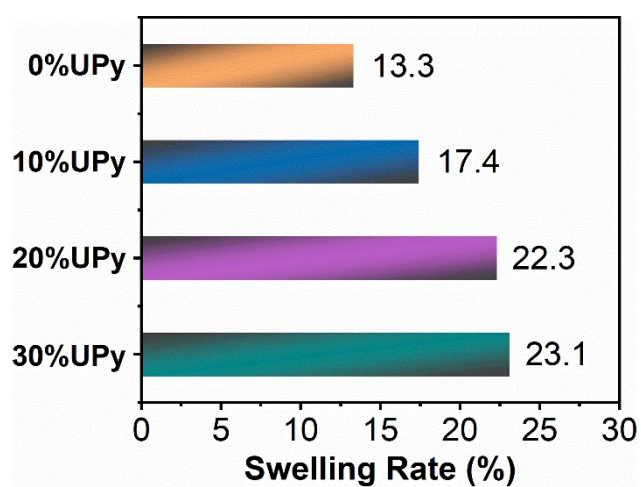
Figure S32. Swelling ratios of the DCPs in methanol.
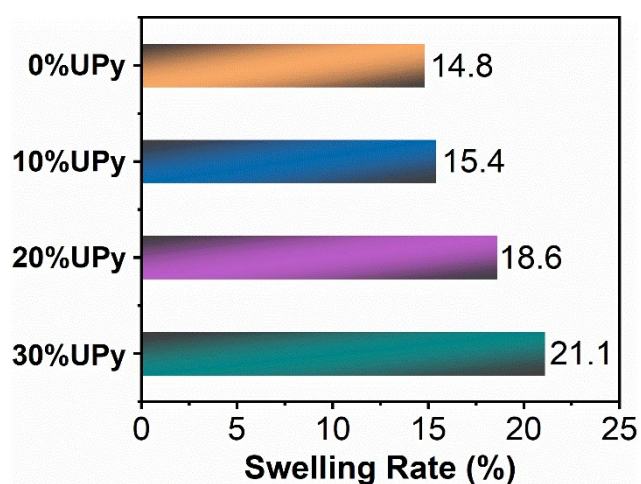
Figure S33. Swelling ratios of the DCPs in ethanol.
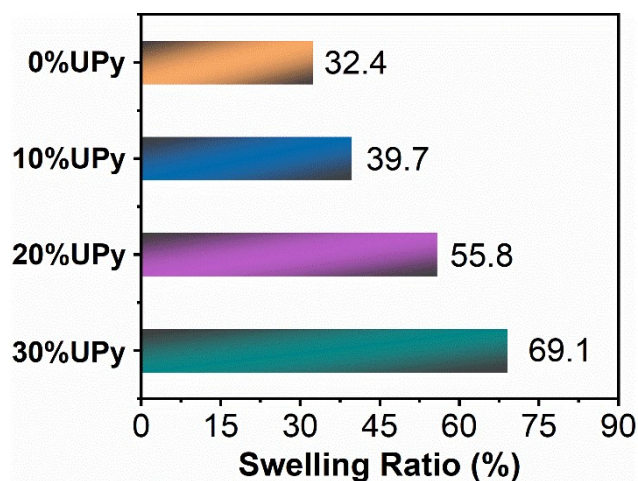
Figure S34. Swelling ratios of the DCPs in chloroform.
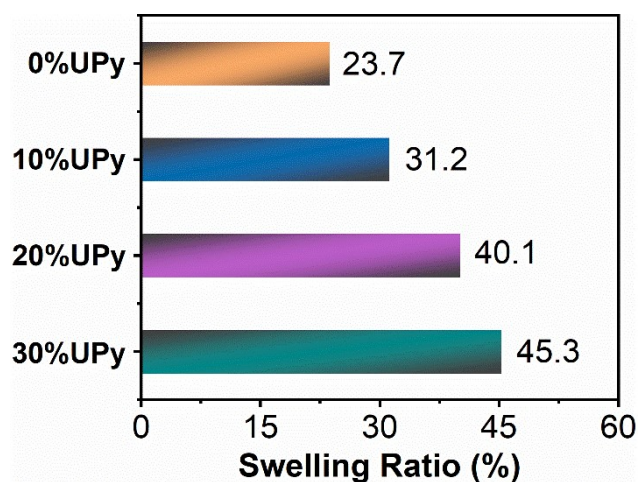
Figure S35. Swelling ratios of the DCPs in DMF.
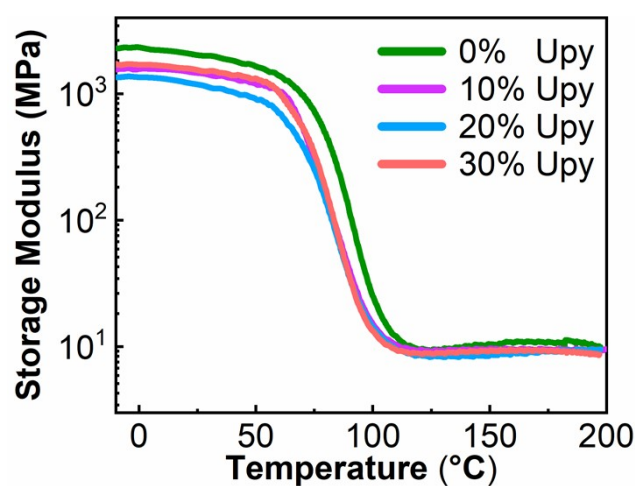
Figure S36. DMA curves of DCPs (storage modulus as a function of temperature).

Table S1. Thermal properties of DCPs.

Sample	T_g (°C)		E' (MPa)	v_e (mol cm^{-3})
	DSC	DMA		
0%UPy	67	94	10.3	970

10%UPy	65	92	9.5	900
20%UPy	66	91	9.2	865
30%UPy	66	91	8.7	819

$$v_e = E'/3RT \qquad (S1)$$

$$T = T_g + 60\ °C \qquad (S2)$$
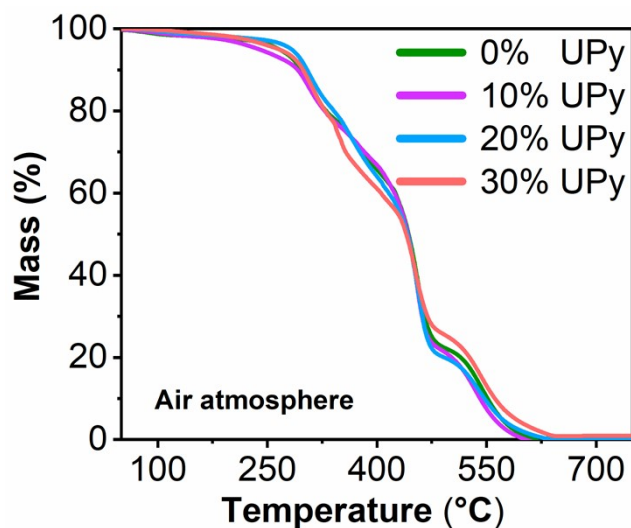
Figure S37. TGA curves of DCPs under air atmosphere.

Table S2. Thermal stability of DCPs.

Sample	$T_{d5\%}$ (°C)		$T_{d30\%}$ (°C)		R_{800} (%)		T_s (°C)	
	Air	N_2	Air	N_2	Air	N_2	Air	N_2
0%UPy	267	272	381	360	0	8.2	164	159
10%UPy	240	258	383	355	0	8.6	160	155
20%UPy	265	282	377	359	0.3	7.4	163	161
30%UPy	266	269	358	347	1.0	9.9	157	155

$$T_s = 0.49[T_{d5\%} + 0.6(T_{d30\%} - T_{d5\%})] \qquad (S3)$$
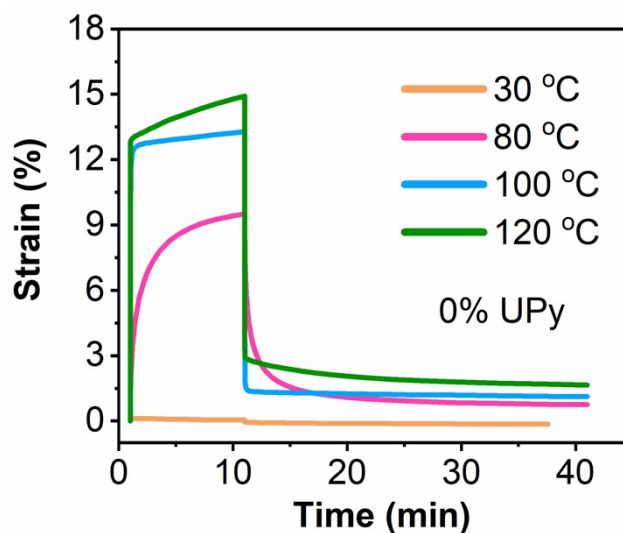
Figure S38. Creep curves of 0%UPy at different temperatures.
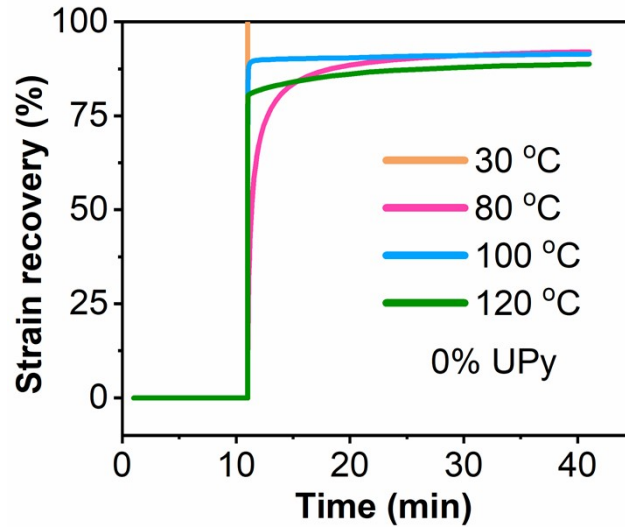
Figure S39. Creep recovery curves of 0%UPy at different temperatures.
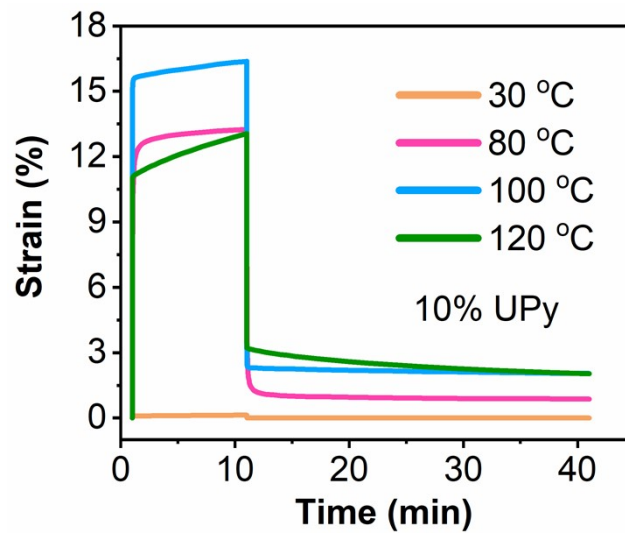
Figure S40. Creep curves of 10%UPy at different temperatures.
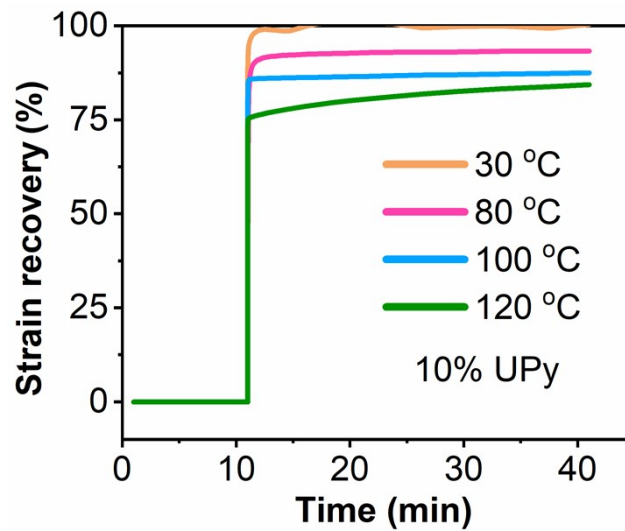
Figure S41. Creep recovery curves of 10%UPy at different temperatures.
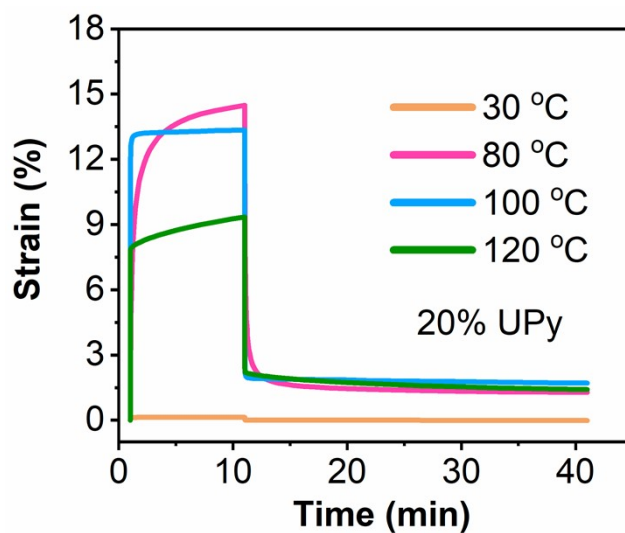
Figure S42. Creep curves of 20%UPy at different temperatures.
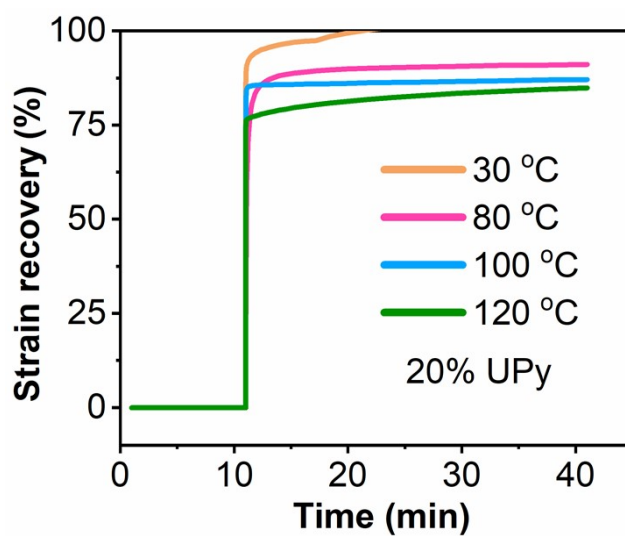
Figure S43. Creep recovery curves of 20%UPy at different temperatures.
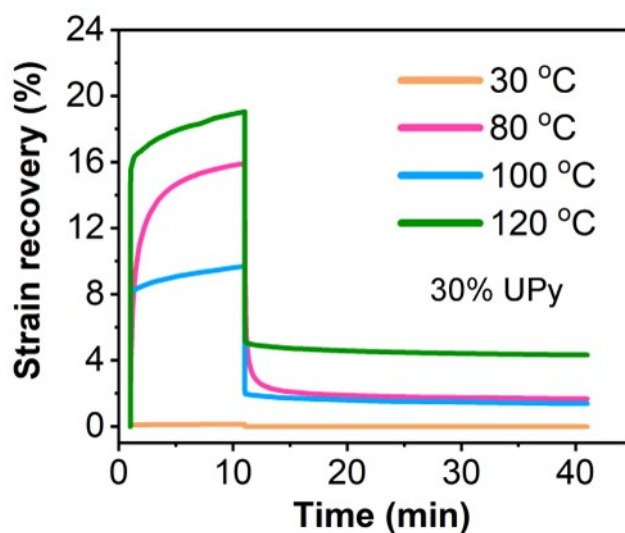
Figure S44. Creep curves of 30%UPy at different temperatures.
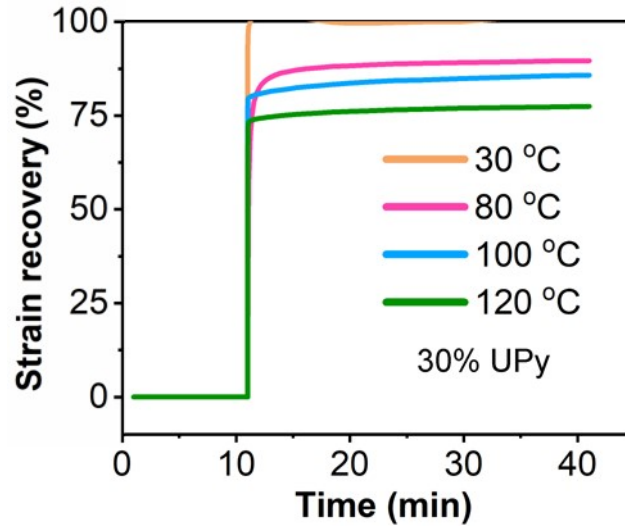
Figure S45. Creep recovery curves of 30%UPy at different temperatures.
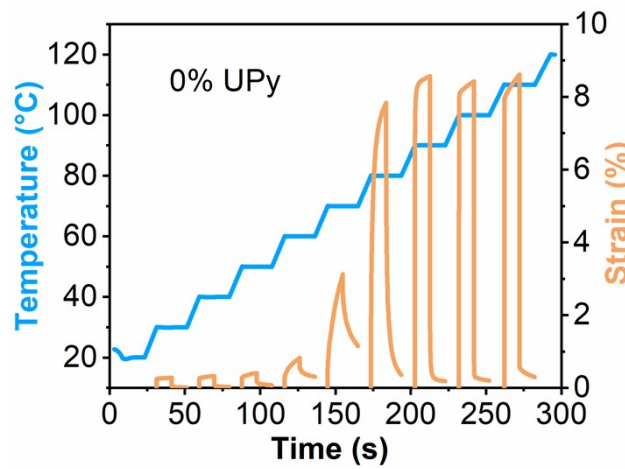
Figure S46. TTS curves of 0%UPy at 20-120 °C.
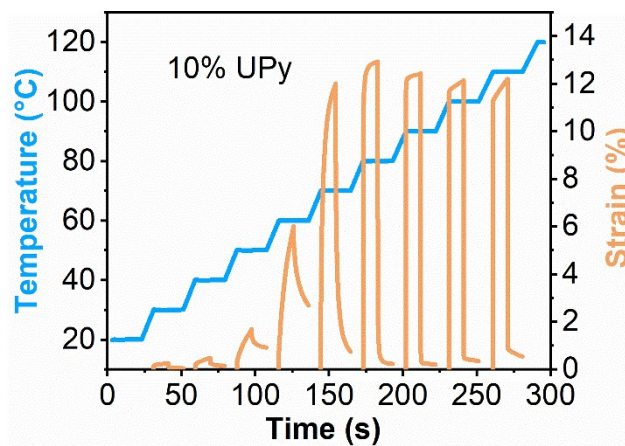
Figure S47. TTS curves of 10%UPy at 20-120 °C.
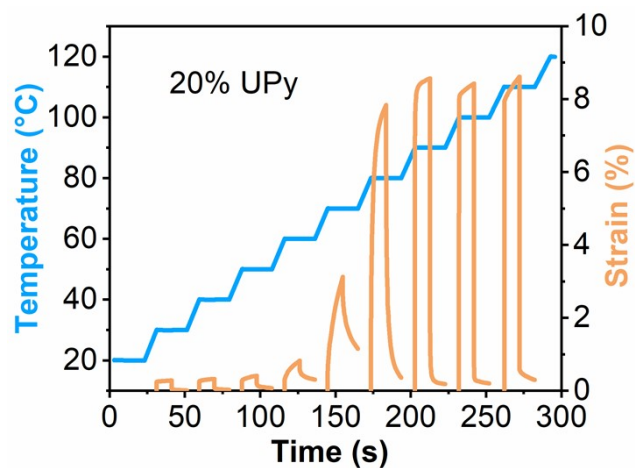
Figure S48. TTS curves of 20%UPy at 20-120 °C.
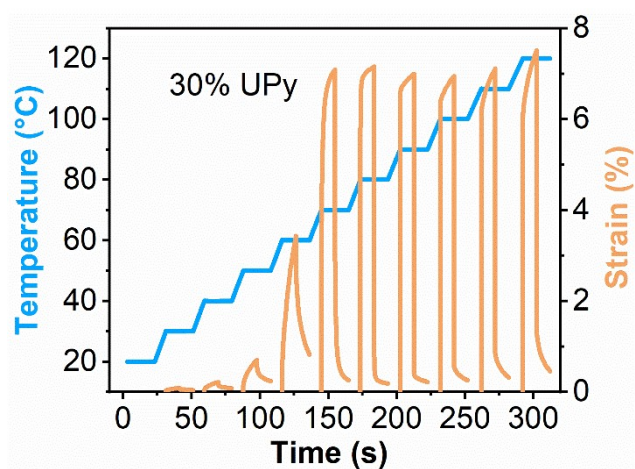
Figure S49. TTS curves of 30%UPy at 20-120 °C.
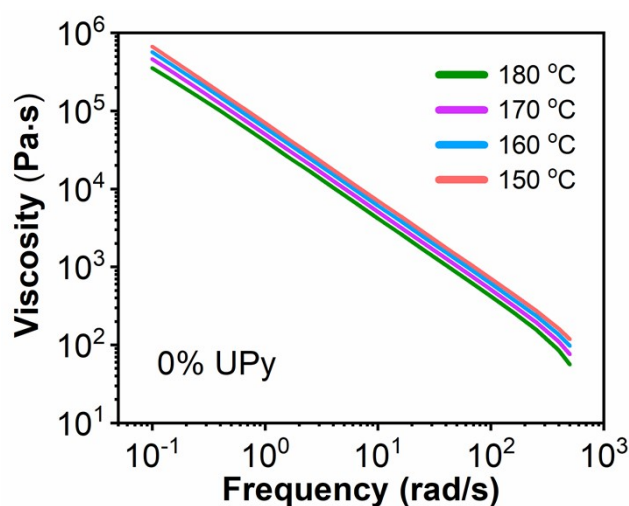
Figure S50. Frequency sweep tests of 0%UPy at different temperatures (viscosity as a function of frequency).
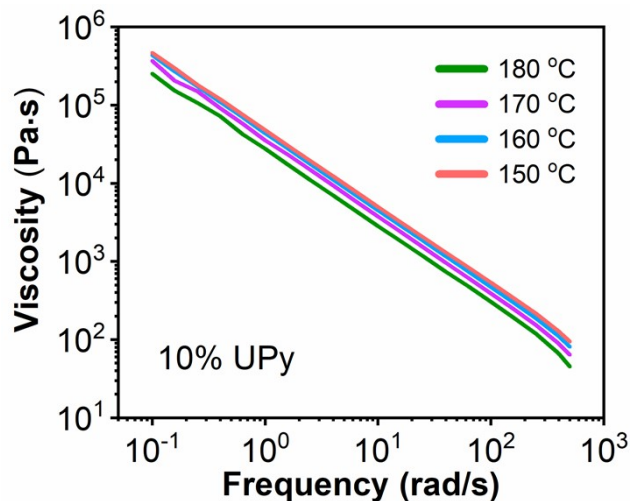
Figure S51. Frequency sweep tests of 10%UPy at different temperatures (viscosity as a function of frequency).
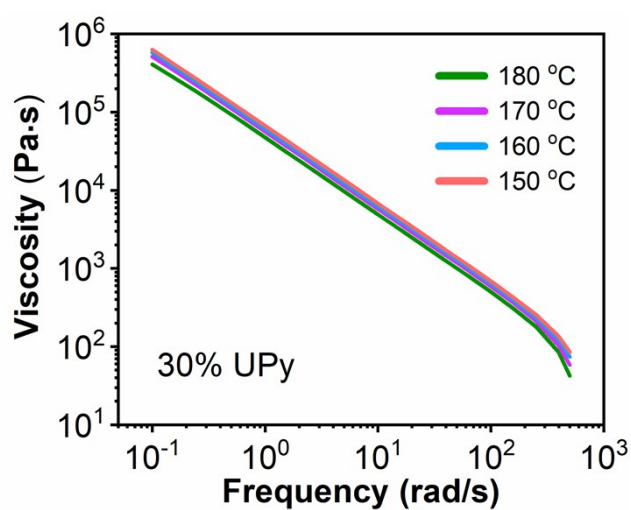
Figure S52. Frequency sweep tests of 30%UPy at different temperatures (viscosity as a function of frequency).
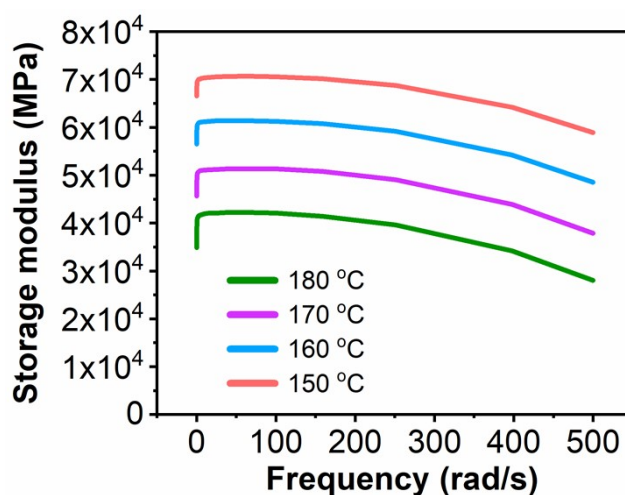
Figure S53. Frequency sweep tests of 0%UPy at different temperatures (storage modulus as a function of frequency).
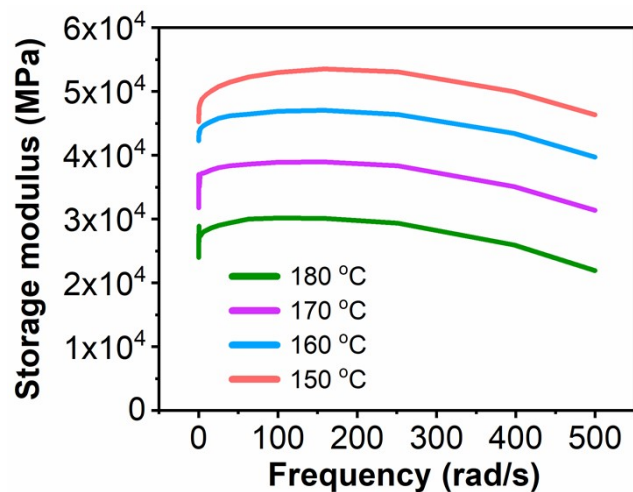
Figure S54. Frequency sweep tests of 10%UPy at different temperatures (storage modulus as a function of frequency).
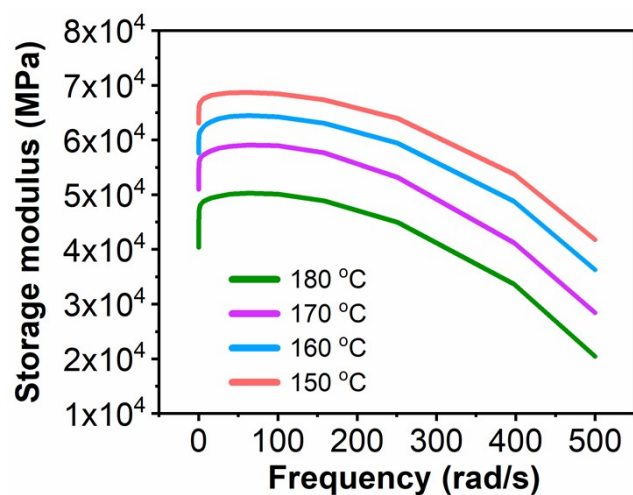
Figure S55. Frequency sweep tests of 30%UPy at different temperatures (storage modulus as a function of frequency).
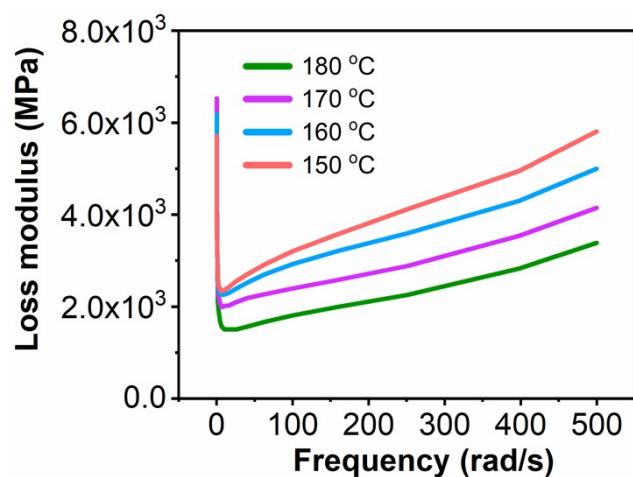
Figure S56. Frequency sweep tests of 0%UPy at different temperatures (loss modulus as a function of frequency).
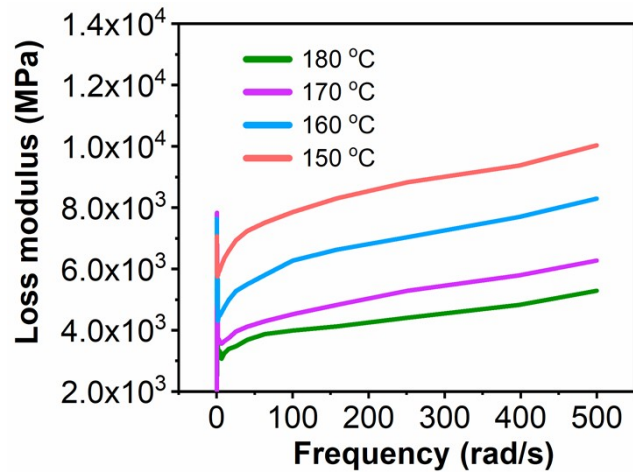
Figure S57. Frequency sweep tests of 10%UPy at different temperatures (loss modulus as a function of frequency).
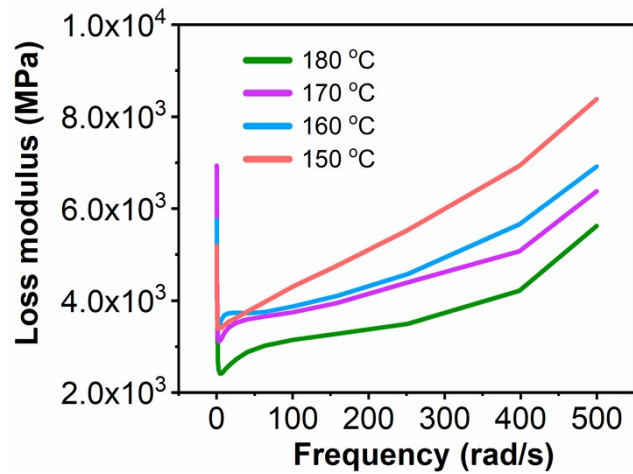
Figure S58. Frequency sweep tests of 30%UPy at different temperatures (loss modulus as a function of frequency).

Reprocessing properties of DCPs
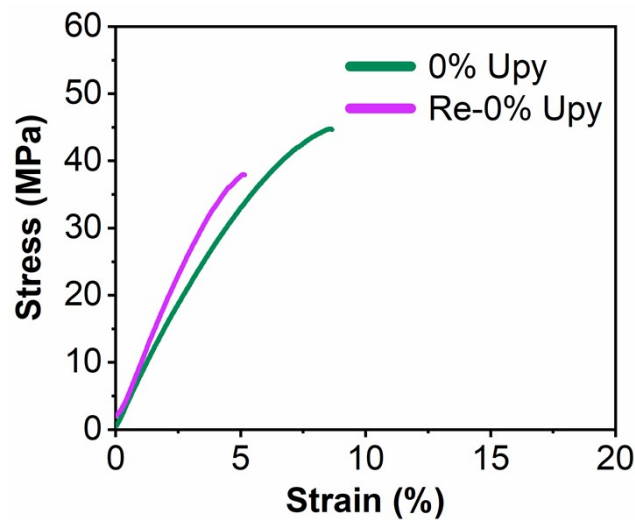
Figure S59. Representative tensile stress-strain curves of 0%UPy before and after reprocess.
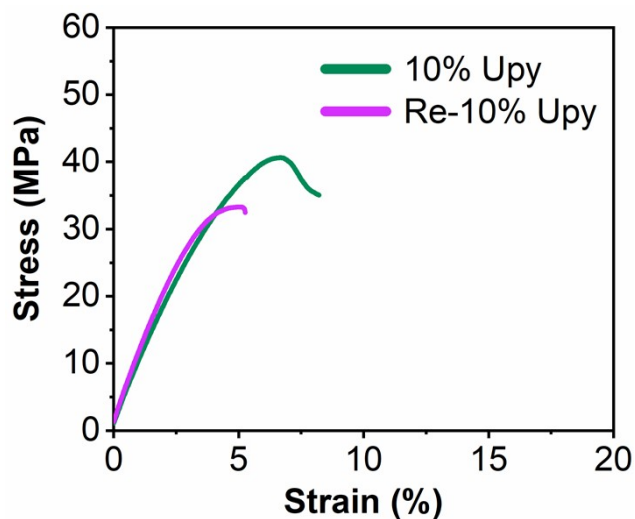
Figure S60. Representative tensile stress-strain curves of 10%UPy before and after reprocess.
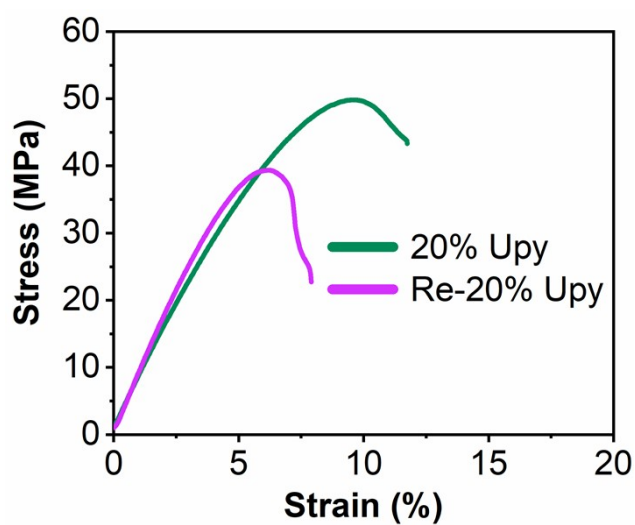
Figure S61. Representative tensile stress-strain curves of 20%UPy before and after reprocess.
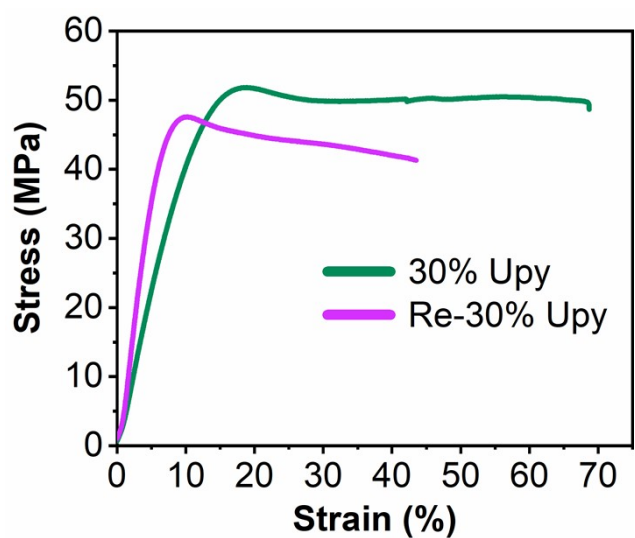
Figure S62. Representative tensile stress-strain curves of 30%UPy before and after reprocess.

Table S3. Mechanical properties of DCPs before and after reprocessing

Sample	Young's modulus (MPa)	Tensile strength (MPa)	Elongation at break (%)
0%UPy	953±23	45±7	8.7±1.3
Re-0%UPy	1107±47	38±6	5.2±0.9
10%UPy	901±18	41±6	8.2±2.1
Re-10%UPy	973±31	33±8	5.3±1.3
20%UPy	828±19	50±11	11.8±2.2
Re-20%UPy	925±39	48±7	8.7±3.1
30%UPy	534±13	52±10	68.7±12.7
Re-30%UPy	637±28	48±12	47.3±13.4
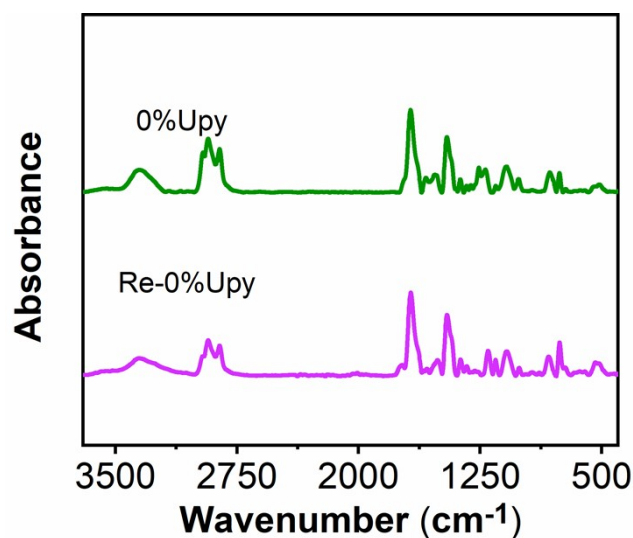
Figure S63. FT-IR spectrum of 0%UPy before and after reprocess.
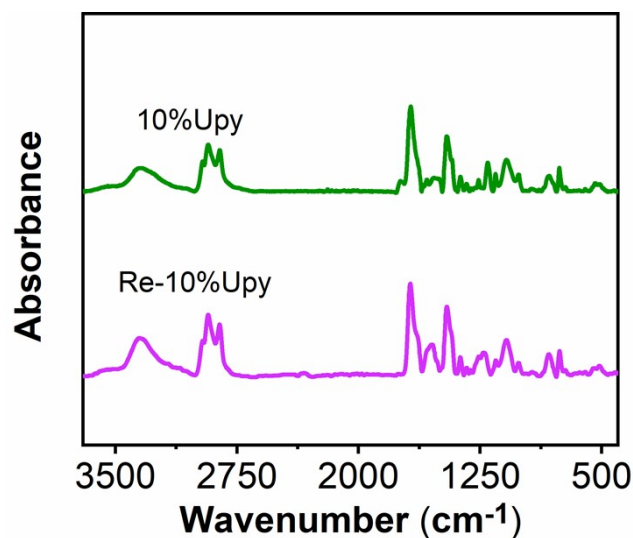
Figure S64. FT-IR spectrum of 10%UPy before and after reprocess.
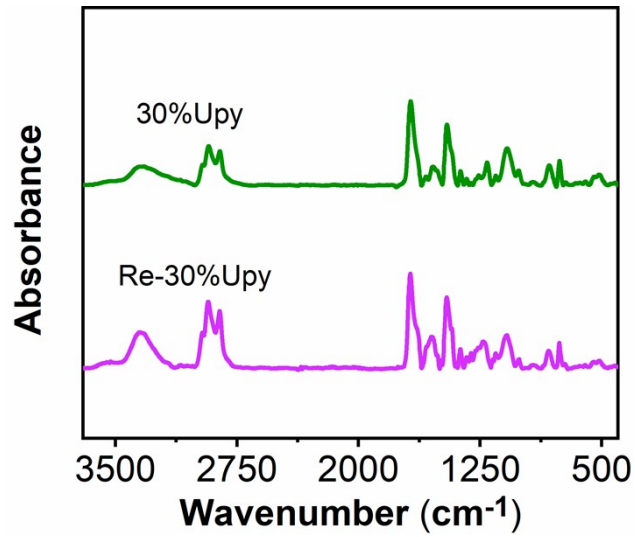
Figure S65. FT-IR spectrum of 30%UPy before and after reprocess.

Preparation of CF/DCP composite
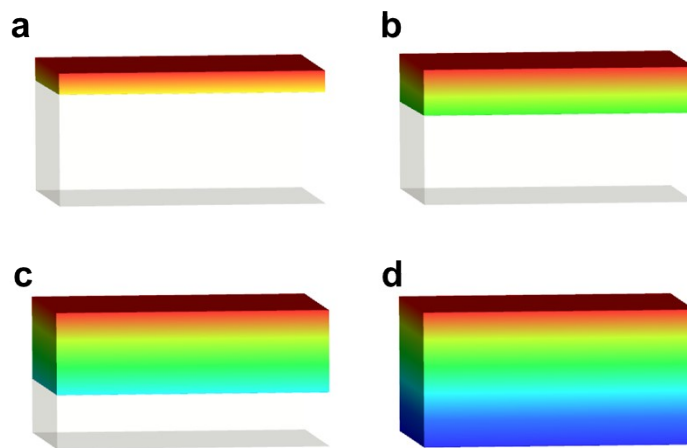
Figure S66. Moldex 3D-simulated flow front of 20%UPy during the preparation of CF/DCP composite at 180 °C, 10 MPa after **a**) 159 s, **b**) 318 s, **c**) 477 s and **d**) 636 s.
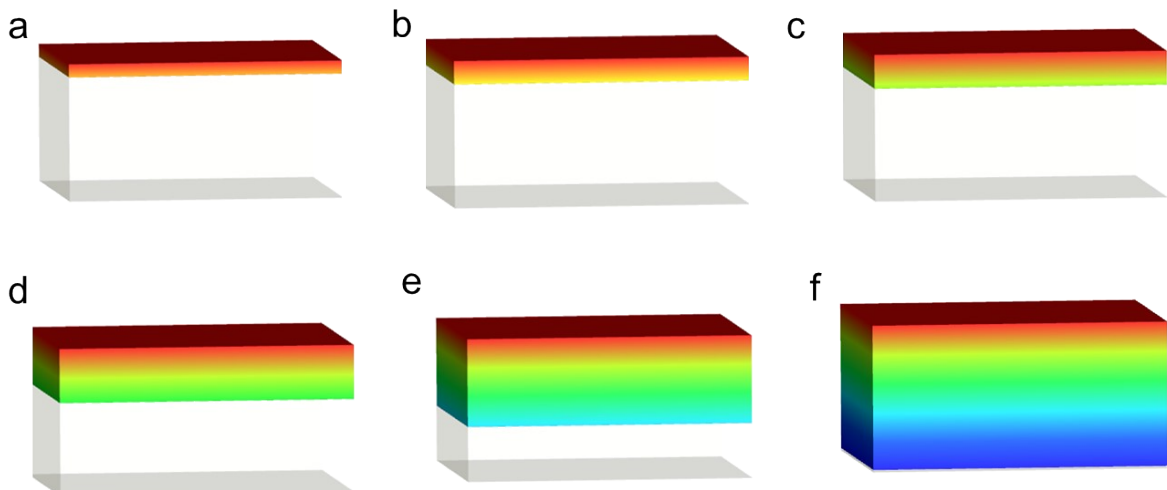
Figure S67. Moldex 3D-simulated flow front of 20%UPy during the preparation of CF/DCP composite at 160 °C, 5 MPa after **a)** 160 s, **b)** 320 s, **c)** 480 s, **d)** 640 s, **e)** 960 s and **f)** 1280 s.
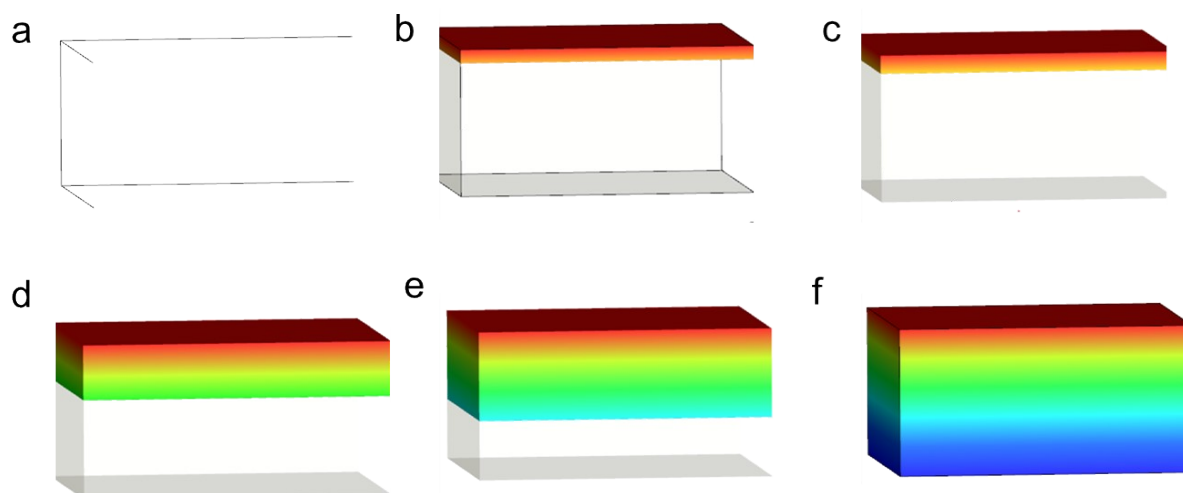
Figure S68. Moldex 3D-simulated flow front of 20%UPy during the preparation of CF/DCP composite at 160 °C, 1 MPa after **a)** 480 s, **b)** 960 s, **c)** 1280 s, **d)** 3000 s, **e)** 4800 s and **f)** 6600 s.
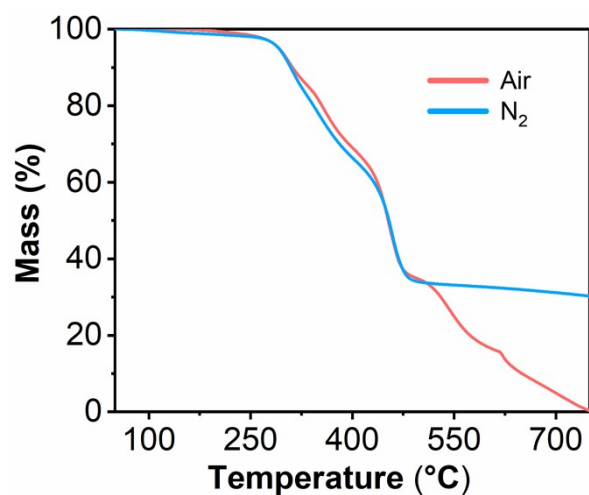
Figure S69. TGA curves of CF/DCP composite under air and N_2 atmospheres.

Table S4. Thermal stability of CF/DCP (20%UPy) composite

Sample	$T_{d5\%}$ (°C)		$T_{d30\%}$ (°C)		R_{800} (%)		T_s (°C)	
	Air	N_2	Air	N_2	Air	N_2	Air	N_2
CF/DCP composite	292	292	395	381	0	30	174	169
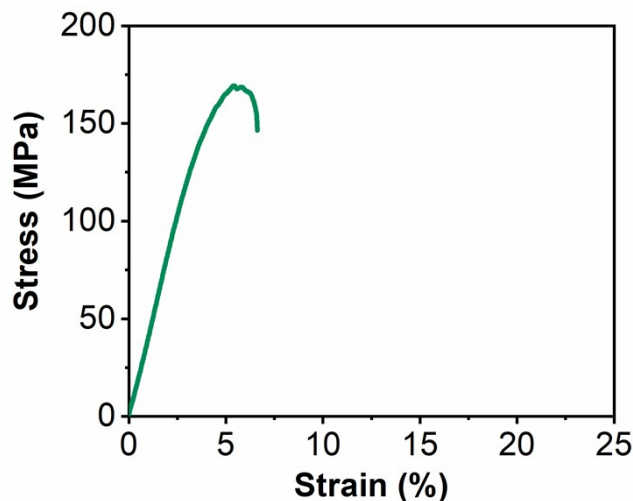
Figure S70. Representative tensile stress-strain curves of CF/DCP (20%UPy) composite.

Table S5. Mechanical properties of CF/DCP (20%UPy) composite

Sample	Young's modulus (MPa)	Tensile strength (MPa)	Elongation at break (%)
CF/ polyurethane composite	4519±167	169±26	6.6±1.9

Reference

1. X. Xu, S. Ma, H. Feng, J. Qiu, S. Wang, Z. Yu and J. Zhu, *Polym. Chem.*, 2021, **12**, 5217-5228.

2. B. Qin, S. Zhang, P. Sun, B. Tang, Z. Yin, X. Cao, Q. Chen, J.-F. Xu and X. Zhang, *Adv. Mater.*, 2020, **32**, 2000096.

3. B. Zhu, Z. Feng, Z. Zheng and X. Wang, *J. Appl. Polym. Sci.*, 2012, **123**, 1755-1763.

4. C. A. Tretbar, J. A. Neal and Z. Guan, *J. Am. Chem. Soc.*, 2019, **141**, 16595-16599.

5. M. Capelot, M. M. Unterlass, F. Tournilhac and L. Leibler, *ACS Macro Lett.*, 2012, **1**, 789-792.

6. R. G. Parr, *Oxford University Press*, 1989, **1**, 1989.

7. C. Lee, W. Yang and R. G. Parr, *Phys. Rev. B*, 1988, **37**, 785.

8. A. Becke, *Chem. Phys.*, 1993, **98**, 5648.

9. K. B. Wiberg, *J. Comput. Chem.*, 1986, **7**, 379-379.